Atmos. Chem. Phys. Discuss., doi:10.5194/acp-2016-681, 2016
Manuscript under review for journal Atmos. Chem. Phys.
Published: 10 October 2016

Identification of dust sources and hotspots in East Asia during 2000-2015: implications for numerical modeling and forecasting

Xuelei Zhang[1, 3]; Daniel Q. Tong[2,8,9]; Guangjian Wu[3]; Xin Wang[4]; Aijun Xiu[1,5]; Yongxiang Han[6]; Tianli Xu[3,7]; Shichun Zhang[1]; Hongmei Zhao[1]

[1] Key laboratory of Wetland Ecology and Environment, Northeast Institute of Geography and Agroecology, Chinese Academy of Sciences, Changchun 130102, China
[2] U.S. NOAA Air Resources Laboratory, College Park, MD 20740, USA
[3] Key Laboratory of Tibetan Environment Changes and Land Surface Processes, Institute of Tibetan Plateau Research, CAS Center for Excellence and Innovation in Tibetan Plateau Earth System Sciences, Chinese Academy of Sciences, Beijing 100101, China
[4] College of Atmospheric Sciences, Lanzhou University, Lanzhou 730000, China
[5] Institute for the Environment, University of North Carolina at Chapel Hill, Chapel Hill, North Carolina, USA
[6] Key Laboratory for Aerosol-Cloud-Precipitation of China Meteorological Administration, Nanjing University of Science Information &Technology, Nanjing, 210044, China
[7] University of Chinese Academy of Sciences, Beijing 100049, China
[8] Cooperative Institute for Climate and Satellites, University of Maryland, College Park, Maryland, MD 20740
[9] Center for Spatial Information Science and Systems, George Mason University, Fairfax, Virginia, VA 22030

Correspondence to: X. L. Zhang (zhangxuelei@neigae.ac.cn) and G. J. Wu (wugj@itpcas.ac.cn)

Abstract

More detailed knowledge regarding recent variations in the characteristics of East Asian dust events and dust sources can effectively improve regional dust modeling and forecasts. Here we reassess the accuracy of previous predictions of trends in dust variations in East Asia, and establish a relatively detailed inventory of dust events based on satellite observations from 2000 to 2015. More than 2000 Moderate Resolution Imaging Spectroradiometer (MODIS) images of 462 sand and dust storm events over East Asia were collected and analyzed, and individual events were tracked back to their sources through a combination of color RGB images, brightness temperature difference, and trajectory simulations using the HYSPLIT model. Decreased dust event frequency in spring but increased frequencies in summer and autumn were observed. Of the identified

Atmos. Chem. Phys. Discuss., doi:10.5194/acp-2016-681, 2016
Manuscript under review for journal Atmos. Chem. Phys.
Published: 10 October 2016

dust emission sources, sandy lands and lake beds, rather than the sandy and stone deserts, were found to be the dominant dust sources. Dust hotspots in East Asia are mainly dry lake and river beds and alluvial fans. Recent changes in land use associated with anthropogenic activities (mining and excessive exploitation of water resources) are revealed as one of the major factors leading to an expansion of dust source regions, especially for the northeastern part of Taklimakan desert. Trajectory analysis also shows that dust can even be transported northwards by the Mongolia Cyclone, to the Far East region and even the Arctic Circle, potentially affecting the climate and ecosystem of the Arctic region. Recent physically-based dynamic approaches adopted in dust models reduce the reliance on empirical source functions in dust modeling; however, the validity of down-scaling these schemes to regional scale needs to be further verified with "ground-truth" information as reported here.

Keywords: dust sources, remote sensing, MODIS, modeling, anthropogenic activities

1. Introduction

Mineral dust is a major component of atmospheric aerosols and affects various aspects of the earth-climate system (Knippertz et al., 2014), including radiation balance (Huang et al., 2006), precipitation (Creamean et al., 2013; Vinoj et al., 2014) and cloud cover (Solomos et al., 2011; Atkinson et al., 2013), Ocean and terrestrial biogeochemical cycles (Maher et al., 2010), air quality and visibility (Wang et al., 2012), and even human health (Goudie et al., 2014). The relative impacts of dust within the land-atmosphere-ocean system depend on physiochemical characteristics such as particle size distribution, morphology, and mineralogy (Formenti et al., 2011b; Mahowald et al., 2011; Zhang et al., 2015b), which, although subject to modification during transport (Formenti et al., 2011a), are functions of the source from which they are derived (Shao et al., 2011; Perlwitz et al., 2015). Furthermore, whether derived directly from the point of origin or re-entrained along its pathway, dust may become mixed with other natural or/and anthropogenic materials, potentially causing further harm to wildlife, plants, and humans.

Knowledge of the specific sources and hotspots (extraordinally active sources) of dust emissions at different geographic scales (global, regional and sub-regional) is crucial for improving the prediction accuracy of dust events by numerical models of climate and air quality (Wang et al., 2012; Heinold et al., 2015). Three approaches are frequently used to identify dust sources: frequency statistics, model simulation, and remote sensing. Given the complexity of dust mobilization processes, analyses of storm frequencies have several weaknesses that may result in uncertainties: observer bias is an intrinsic limitation, and the correlation between dust storm frequency and dust sources is not necessarily direct, because both transported dust and locally raised dust can reduce visibility. Numerical modeling is another popular method of identifying dust sources (e.g., Ginoux et al., 2001; Park et al., 2010), but this method is crucially dependent on the parameterization of dust emissions. Different initial inputs will result in variations in source identification. To improve numerical dust models, obtaining more detailed information on dust emission sources is crucial. The newly implemented Saharan source maps, based on sources directly identified by satellites, have been adopted to verify improvements in dust models (Parajuli et al., 2014; Heinold et al., 2015).

Since surface observations are generally sparse in desert regions, it is difficult to locate dust emission sources and subsequent dust trajectories following a dust outbreak. This problem of coarse horizontal-resolution observations can be overcome with the aid of satellite remote sensing. Data from AVHRR (Tegen and Fung, 1995), POLDER (Deuze et al., 2001), TOMS (Prospero et al.,2002), MODIS (Ginoux et al., 2012; Vickery et al., 2013), SeaWiFS (Eckardt and Kuring, 2005), GOES (Wang et al., 2003), MISR (Kalashnikova et al., 2005), SEVIRI (Ashpole and Washington, 2013), OMI (Bryant et al., 2007), AIRS (DeSouza-Machado et al., 2010) and IASI (Klüser et al., 2011) have been successfully used for dust monitoring and source identification. Satellite imaging can also be used for dust modeling and forecasting, now that long-term satellite data on dust storms are available. However, there are constraints to identify dust sources using satellite imaging. Polar orbiting satellites typically collect only one snapshot per day, which may introduce temporal and spatial biases in source detection; for example, the aerosol index from TOMS or OMI may not be used to determine dust origin sources (Darmenova et al., 2005; Baddock et al., 2009).

Atmos. Chem. Phys. Discuss., doi:10.5194/acp-2016-681, 2016
Manuscript under review for journal Atmos. Chem. Phys.
Published: 10 October 2016

At the global scale, a low-resolution (2.5°) map of dust sources estimated from the TOMS Aerosol Index has lead to measurable improvements in modeling global distribution of dust emissions (Ginoux et al., 2001), and more recently a synthesis of global-scale high-resolution (0.1°) dust source locations has been developed based on MODIS Deep Blue AOD products which consider potential anthropogenic dust emissions (Ginoux et al., 2012). Engelstaedter and Washington (2007) correlated the TOMS Aerosol Index with wind speed and gustiness, and identified 131 global hotspots of dust emissions during 1984 to 1990. Nine of these were located in East Asia, but due to the coarse resolution their spatial coverage was uncertain and there is limited geomorphological understanding of these sources. It is clear that inherent seasonal and diurnal dust emission variations, along with the spatial heterogeneity of dust sources in global and mesoscale models, are poorly constrained due to inaccurate source alocation and quantification (Uno et al., 2006). Average aerosol optical depth (AOD) over a long time series has been used to detect persistent, regional-scale dust sources (e.g. Ginoux et al., 2012), but accurate and event-specific source identification requires clear delineation of the upwind margin of the plumes. However, it is apparent that the detection of spatially discrete and intermittent sources can be undertaken using moderate resolution polar-orbiting data, and a few studies have focused on detection techniques or compilation of regional hotspots worldwide: for example, in Australia (Baddock et al., 2009), the Middle East (Karimi et al., 2012; Jafari and Malekian, 2015), Africa (Knippertz and Todd, 2010; Ashpole and Washington, 2013; Vickery et al., 2013), North America (Rivera et al., 2010; Lee et al., 2012) and Central Asia (Nobakht et al., 2015). More recently, dry lakes, riverbeds, mines and croplands contributing to dust emissions over eastern East Asia have been identified as hot spots on the basis of high-resolution MODIS images (Zhang et al. 2015a). Nevertheless, an inventory of dust sources and hot spots based on satellite observations at the sub-basin scale is still nonexistent for East Asia as a whole.

Furthermore, it is well known that there is considerable interannual variability in dust emission and transport, and several studies have predicted future variability on the basis of different analyses. Based on the significant negative correlation between surface air temperature around Lake Baikal and dust storm frequency, Zhu et al. (2008) demonstrated that the future dust storm frequency in spring over the East Asia was anticipated to continuously decrease after the year 2007. Meanwhile, another forecast predicted that sandstorm occurrence in northern China will increase gradually, entering a new, relatively active period (Li and Zhong, 2007). Obviously, large discrepancy and uncertainties still remain in the predications, and there is need to collect more ground- or satellite-based observations to assess the directionality and accuracy of the prediction. Such assessment can be also be used to re-evaluate and improve our knowledge on regional dust emission and transport by air quality and climate models.

The goals of the research presented in this paper are twofold. First, it will provide a unified, regional and sub-regional dust sources and hot spots inventory for East Asia, to improve numerical modeling of dust emission and transport, and to consider measures to mitigate wind erosion. Second, this study will present annual and seasonal variations of dust events for the period of 2000-2015 to reassess past predictions and improve our knowledge on the regional patterns of dust emission.

This paper is structured as follows. Section 2 describes the satellite platforms and observation data, the analysis method and the numerical models. In Section 3, we demonstrate the interannual variations of dust emissions and the distribution of dust hotspots. Relationships with climate indices and implications for dust numerical prediction are then discussed in Section 4. Finally, Section 5 presents our conclusions.

2. Data and methods

2.1 Data

MODerate Resolution Imaging Spectroradiometer (MODIS) collects observations in 36 spectral bands with wavelengths from 0.41 to 14.4 µm and nadir spatial resolutions of 1 km, 0.5 km, and 0.25 km. It is currently operating onboard the NASA Earth Observing System (EOS) Terra and Aqua satellites, launched in December 1999 and May 2002, respectively. The higher temporal and spectral resolutions of MODIS improve its dust identification capability over those of previous-generation earth-observing systems. Daily MODIS Level 1B (L1B) 1 km data (MOD021KM=Terra, and MYD021KM=Aqua) used in this work have been processed to convert the sensor's on-orbit responses in digital numbers to radiometrically calibrated and geo-located data products (v5.06 processing for Terra and v5.07 for Aqua). Data were obtained from the National Snow and Ice Data Center (NSIDC; http://nsidc.org/) and the Level 1 and Atmosphere Archive and Distribution System (LAADS; http://ladsweb.nascom.nasa.gov/). Daily MODIS Level 2 Aerosol data are available as a 10 × 10 km resolution (at nadir) pixel array. There are two MODIS Aerosol data product file types: MOD04_L2, containing data collected from the Terra platform and MYD04_L2, containing data collected from the Aqua platform. Here we only use the MYD04 Aqua product because Deep Blue (see below) retrievals are not yet available for MOD04 Terra data. Improvements in the surface reflectivity retrieval and algorithm mean that Collection 6 MODIS Deep Blue aerosol products, both absolute AOD and its spectral variation, have changed since Collection 5.1 (Sayer et al., 2013). Details of the remote sensing data are outlined in Table 1.

Table 1 Detailed spatial and temporal information of remote sensing data used for dust detection in this study

Satellite Data	Data level	Spatial resolution (km)	Archive length	Local overpass time
MOD02 [Terra]	L1B	0.25×0.25 (VIS) 0.5×0.5 (VIS+NIR) 1×1(TIR+all bands)	1999 to date	10:30 AM
MYD02 [Aqua]	L1B	0.25×0.25 (VIS) 0.5×0.5 (VIS+NIR) 1×1(TIR+all bands)	2002 to date	13:30 PM
MYD04 [Deep Blue]	L2	10×10	2002 to date	13:30 PM

On the basis of statistical information on dust events obtained from the China Meteorological Administration and local dust storm forecasting (http://www.duststorm.com.cn), we acquired MODIS images of eastern Asia (70–140°E, 20 – 60°N) from NSIDC and LAADS, NASA. In more than 6000 images, we analyzed 214 regional and transported dust events (total 2374 MODIS images and HDF format data files) covering the years 2000 to 2015, including all the dust storms identified by Zhang et al. (2008) for the period 2000 to 2006 and by Kim and Lee (2013). In order to build a plume and source location inventory for East Asia, images were visually examined for dust plumes. After identifying a MODIS image containing dust, we searched forwards and

Atmos. Chem. Phys. Discuss., doi:10.5194/acp-2016-681, 2016
Manuscript under review for journal Atmos. Chem. Phys.
Published: 10 October 2016

backwards (temporally) in our study domain for other images to build a scene for each dust event (including formation, development, dispersal, transportation); for inclusion in the inventory all dust storms needed to be present in at least two satellite images. Dust plumes occurring underneath clouds are unlikely to be detected. Not all plumes were observed to be attached to a source but could still be attributed to likely emission points based on back trajectory analysis.

2.2 Dust detection algorithm

As advised by Baddock et al. (2009), at the regional scale, dust events can be detected using MODIS AOD or OMI AI products. If either of these two products indicates the presence of dust, then there is the potential for determining dust sources at higher resolution. The MOD/MYD04 aerosol products provide data processed to a common standard that enables comparison from one region to another. The versatile MOD/MYD02 data can be processed simply by using brightness temperature difference to enhance the dust signal. Where cloud is present, or if it is necessary to highlight the dust plume, then one of the methods for employing a dust/non-dust threshold can be used, but it is recommended that event-specific thresholds are calculated manually (as opposed to uniform regional thresholds). The algorithm for the higher resolution technique based on satellite data is illustrated in Figure 1.

The ability to use remotely-sensed data both to detect a dust plume and to identify the location from which it has originated is affected by several factors including the radiative transfer properties of the material emitted, the radiative properties of the ground/ocean surface over which the plume is transported, the size and density of the dust plume, the time of satellite overpass relative to dust emission, the presence or absence of cloud, the horizontal and vertical plume trajectory, and the sensor characteristics and radiative transfer model used to detect dust.

Atmos. Chem. Phys. Discuss., doi:10.5194/acp-2016-681, 2016
Manuscript under review for journal Atmos. Chem. Phys.
Published: 10 October 2016

Atmospheric Chemistry and Physics Discussions

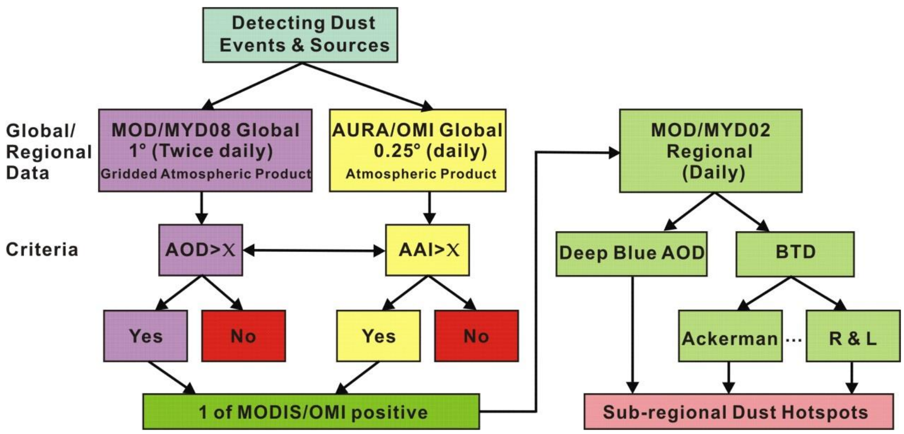

Figure 1 Flowchart of dust detection algorithms used for satellite data in sub-regional scale

Many previous studies have proposed approaches to discriminate airborne dust over bright land surfaces (Ackerman, 1997; Baddock et al., 2009), including the use of true color images, ultraviolet band absorption (Washington et al., 2003), thermal infrared techniques (Ackerman, 1997), and other more complicated algorithms. Both visible bands (VIS) and infrared bands (IR) (often combined) can be used to discriminate dust. When the dust layer is optically thick, the dust particles cause a negative brightness temperature difference (BTD). It has been shown that the BTD methods are the most consistently reliable technique for dust source identification over bright surfaces (Karimi et al., 2012; Baddock et al., 2016). Thus, IR bands (band 31 and band 32) of the MODIS onboard Aqua and Terra satellites are used to detect dust sources over East Asia in this study.

In order to select a fast and effective algorithm to detect massive dust events with different intensities, we reviewed the mainstream "split windows" algorithms for dust detection (Table 2). Note that some algorithms have not been used in the East Asia region. After detailed comparisons and evaluation of different algorithms to detect our pre-selected moderate dust event (May 11, 2011) over East Asia, Method 4, which combined visible bands and infrared bands, was selected as being the most suitable algorithm for differentiating dust from land and clouds in this study (Figure 2). This selection is consistent with Baddock et al. (2009) who concluded that both Methods 1 and 4 worked well for dust source determination over Australia. Method 5 is extremely useful

Atmos. Chem. Phys. Discuss., doi:10.5194/acp-2016-681, 2016
Manuscript under review for journal Atmos. Chem. Phys.
Published: 10 October 2016

Atmospheric Chemistry and Physics
Discussions
Open Access

for visualizing dust, but there are significant problems with precise source identification and determination of dust plume extent.

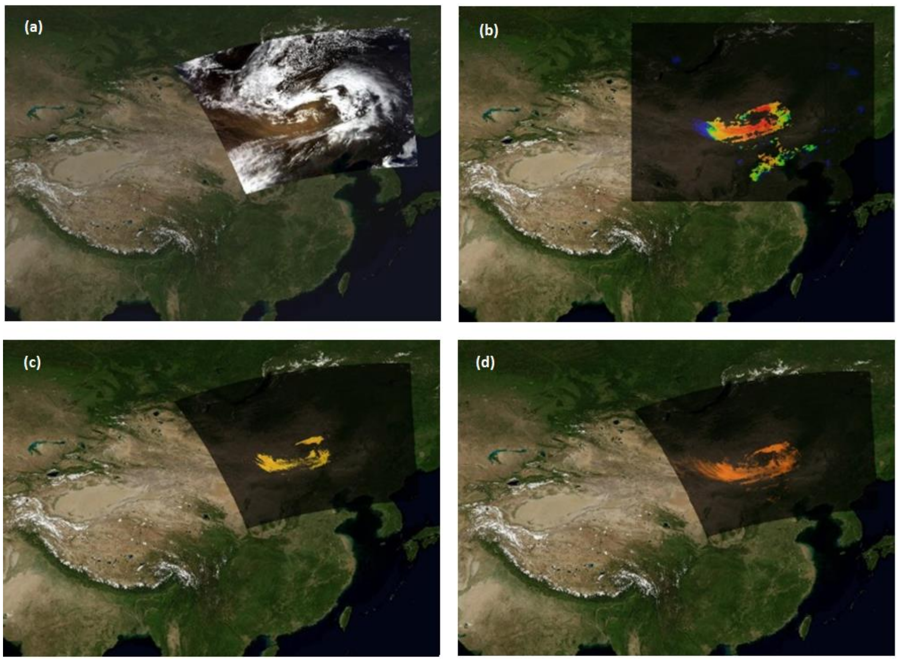

Figure 2. Comparison and evaluation of different algorithms applied to detect a pre-selected moderate dust event (May 11, 2011) over East Asia. (a) True color; (b) Retrieved AOD; (C) BTD method of Ackerman; (d) BTD method of Roskovensky and Liou.

For the majority of events and algorithms, the published or indicative thresholds under-perform and the values vary from event to event. This makes it difficult to suggest appropriate regional scale thresholds and each event was manually adjusted in this study. While some of this variation is due to factors specific to the algorithms or individual events, other factors such as diurnal and seasonal variations in surface temperature/dust contrast (which affect BTD) will affect all the methods.

Once a dust event was determined, it was numbered and classified as either a local or regional transported dust event. Then, all the dust plumes in this event were recorded and the locations (points or/and polygons) of hot spots for dust emission were noted.

Table 2 Summary of dust detection algorithms applied to MODIS L1B data.

Algorithm	Detection threshold	Reference
Method (1):		
$\mathrm{BTD} = BT_{31} - BT_{32}$	$\mathrm{BTD} < \mathrm{constant}$	Ackerman, 1997
Where:	$(-1 \text{ to } 0.5\mathrm{K})$	
$BT_{31} = BT_{10.78-11.28\ \mu m}$		
$BT_{32} = BT_{11.77-12.27\ \mu m}$		
Method (2):		
$\mathrm{BTD} = BT_{31} - BT_{32}$	$\mathrm{BTD} < -0.5\mathrm{K}$	Zhang et al., 2006
$\mathrm{BTD}^{*} = BT_{29} - BT_{31}$	$\mathrm{BTD}^{*} < 0\mathrm{K}$	
Where:		
$BT_{29} = BT_{8.40-8.70\ \mu m}$		
$BT_{31} = BT_{10.78-11.28\ \mu m}$		
$BT_{32} = BT_{11.77-12.27\ \mu m}$		
Method (3):		
$\mathrm{BTD} = BT_{31} - BT_{32}$	$\mathrm{BTD} < -0.5\mathrm{K}$	Karimi et al., 2012
$\mathrm{MEDI} = (BT_{31} - BT_{29})/(BT_{32} - BT_{29})$	$\mathrm{MEDI} < 0.6$	
Where:		
$BT_{29} = BT_{8.40-8.70\ \mu m}$		
$BT_{31} = BT_{10.78-11.28\ \mu m}$		
$BT_{32} = BT_{11.77-12.27\ \mu m}$		
Method (4):		
$\mathrm{BTD} = \exp\{-[\alpha \cdot (R_4/R_{16}) + (BT_{11} - BT_{12}) - \beta]\}$	$\mathrm{BTD} > 1.0$	Roskovensky and Liou, 2005
Where:		
$\alpha = \text{scaling factor } (0.8)$		
$\beta = \text{btd offset } (2.0)$		
$R_4 = R_{0.545-0.565\ \mu m}$		
$R_{16} = R_{0.862-0.877\ \mu m}$		
$BT_{31} = BT_{10.78-11.28\ \mu m}$		
$BT_{32} = BT_{11.77-12.27\ \mu m}$		
Method (5):		
$\mathrm{BTD} = [(BT_{31} - BT_{32})^a + (2R_1 - R_3 - R_4 - BT_{31})^b - (R_{26})^c + (1 - BT_{31})^d]$	$1.3 < \mathrm{BTD} < 2.7$	Miller, 2003
Where:		
$R_1 = R_{0.620-0.670\ \mu m}$		
$R_3 = R_{0.459-0.479\ \mu m}$		
$R_4 = R_{0.545-0.565\ \mu m}$		
$R_{26} = R_{1.360-1.390\ \mu m}$		
$BT_{31} = BT_{10.78-11.28\ \mu m}$		
$BT_{32} = BT_{11.77-12.27\ \mu m}$		
$a = -2 \ to\ 2$		

$b = -1.5\ to\ 0.25$

$c = 0\ or\ 1$

$d = occurrences\ of\ BT_{31\_max}$

2.3 Analysis of transport trajectories

By using the discrimination method described above, we identified dust sources/hotspots and transport by monitoring dust progression as observed in time-series of MODIS images during a dust event. Then, we reconstructed the air-mass trajectories responsible for the dust transport, to validate the dust origins and transport trajectories determined by satellite remote sensing.

Efficacies of four large-scale Lagrangian dispersion models (CALPUFF v5.8, FLEXPART v6.2, SCIPUFF v2.303 and Hybrid Single-Particle Lagrangian Integrated Trajectory (HYSPLIT) model v4.8) were compared, and the National Oceanic and Atmospheric Administration (NOAA) HYSPLIT model has the best performance according to four statistical scores (Anderson and Brode, 2010). Thus, we decided to use it here to calculate three-dimensional trajectories of each transported dust event over a 15-year period from 2000 to 2015. Forward trajectories for all detected dust events were obtained from the National Centers for Environmental Prediction/National Centre for Atmospheric Research reanalysis data (NCEP/NCAR; http://rda.ucar.edu/datasets/ds090.0/). Trajectory starting locations were determined by central coordinates of identified point or/and polygons. Model vertical velocity used the meteorological model's vertical velocity fields, and the trajectory was simulated at 3 starting heights (500, 1000 and 1500 m above mean sea level) for each transported dust event.

3. Results and Discussion

3.1 Interannual and seasonal variations of dust events

Following the analysis of MODIS images we identified 462 dust events and 214 long-lived (>48 hours) dust events during 2000-2015 (Table 1 in the appendix). The frequencies and timing of dust emissions have changed markedly over the past 16 years (Figure 3a). From 2000 to 2002, the study area experienced many dust events, with over 10 dust storms per year. More favorable conditions prevailed in 2003 and 2004. A dustier

Atmos. Chem. Phys. Discuss., doi:10.5194/acp-2016-681, 2016
Manuscript under review for journal Atmos. Chem. Phys.
Published: 10 October 2016

Atmospheric Chemistry and Physics
Discussions
Open Access

period followed from 2005-2007, when 10 long-lived dusts were tracked by MODIS. Between 2005 and 2014, the frequency of severe dust events fluctuated between 10-20 counts per year, with a slightly increasing trend overall.

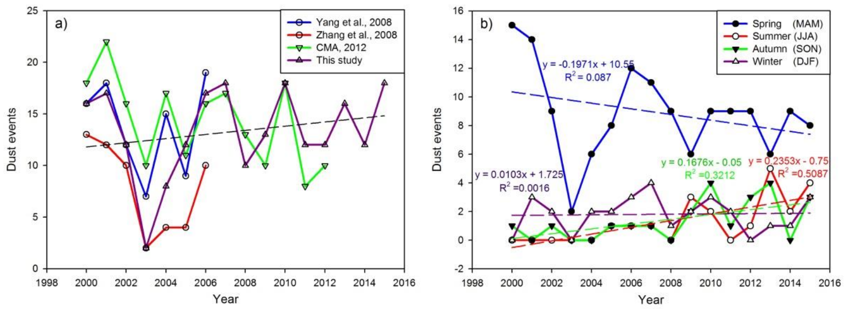

Figure 3. Annual variation (a) and seasonal variation (b) of long-lived dust frequency observed by MODIS during 2000 - 2015

Figure 3b illustrates that most dust events occurred in spring, from March to May, at a clearly decreasing frequency. Since 2008, the increased frequencies of Asian dust events in summer and autumn have been comparable or slightly greater than those in the winter months (i.e. December, January and February). Source regions were mostly located in Inner Mongolia and Northeastern China (named as Manchuria in Table 1 in the appendix), which is consistent with the results of Lim and Chun (2006) and Kim and Lee (2013). The annual frequency of Asian dust events in winter remained stable but with fluctuations (0-4 counts) over the period 2000-2014. Our statistical results based on satellite retrievals show fluctuations corresponding to those in ground-based observations (Yang et al., 2008 and official reported data from CMA), but higher than those in statistical results of transported dust events in satellite retrieves over East Asia (Zhang et al., 2008).

The periodicity of transported dust storms was analyzed using power spectrum analysis from 2000 to 2015 in East Asia which revealed a cyclical period of 3-5 years. This period is consistent with the calculated short cycles (3-4 years) that correspond with the period of El Nino and Southern Oscillation (Littmann, 1991; Wang et al., 2005; Hara et al., 2006; Lee et al., 2015). A long period of 11-12 years corresponding to the sunspot cycle was also identified in the dust storm frequency time series for Asia and Middle East (Wang et al., 2005; Li and Zhong, 2007; Mohammed et al., 2010). Due to our limited data (16 years), this long cycle cannot be identified in our power spectrum analysis; however, an obvious, long-period cycle can be seen through visual inspection, with troughs in 2003 and 2014.

The variations in dust events appear to be controlled by atmospheric dynamics (temperature, precipitation, wind velocity, Mongolia cyclone, polar vortex and Arctic Oscillation), land surface characteristics (soil moisture, desertification, vegetation) and human activities. Several studies have found that dust storm frequency has decreased over East Asia during the past 60 years (Wang et al., 2005; Ding et al., 2005). Since the late 1970s, both observations and simulations have shown that the magnitudes of dust events (both in terms of dust frequency and dust concentration) have been decreasing over the western part of Northern China (Shao et al., 2013; Guan et al., 2015), and even the Tibetan plateau (Han et al., 2008; Kang et al., 2016), except for the Taklimakan desert (Mao et al., 2011, Tan et al., 2014; Yang et al., 2015). However, an increasing trend was detected in the eastern part of Northern China (Lee et al., 2011; Gao et al., 2012; Tan et al., 2014), and in the whole of Mongolia (Lee et al., 2011; Kurosaki et al., 2011).

In addition to the contraction of the Gobi Desert (Sternberg et al., 2015) and the overgrazing-driven expansion of the Hunsandak Desert and the Horqin Desert in the past 16 years (Gao et al., 2012; Tan et al., 2014), precipitation is also an important factor affecting dust events. Records show that rainfall has increased over the past half century in northwestern China, while rainfall has decreased over Mongolia and Eastern Inner Mongolia since the 1990s (Ding et al., 2005; Kurosaki et al., 2011; Gao et al., 2012). Furthermore, Wang et al. (2006) reported that dust storm frequency was low in the eastern part of Northern China, where there are high levels of human activity, indicating that intensive land use did not contribute to dust storm occurrence. However, land use change has been found to be a major factor influencing changes in dust storm frequency in Xinjiang and Northeast China (Tan et al., 2014). Thus, what is the true impact of human activity on regional dust emission in the past 16 years? This question will be further investigated at the sub-regional scale with the assistance of high-resolution satellite images in Section 3.3.

Atmos. Chem. Phys. Discuss., doi:10.5194/acp-2016-681, 2016
Manuscript under review for journal Atmos. Chem. Phys.
Published: 10 October 2016

Atmospheric Chemistry and Physics
Discussions

3.2 Distribution of dust sources at the regional scale

In recent years, identifications of dust sources in East Asia have been mainly conducted on global or/and regional scales. Furthermore, different techniques and methods (compilation of literatures, field investigation, geochemical analysis, satellite observation and numerical modeling) have been applied to accurately locate the dust sources (Xuan et al., 2004; Zhang et al., 2006; Kim and Lee et al., 2013) and to quantify the effects of climate change and anthropogenic activities on dust emissions. In contrast to former studies, the sub-regional scale (for dust sources) and fine scale (for hotspots) were adopted in this paper to establish a more comprehensive source map for dust emission.

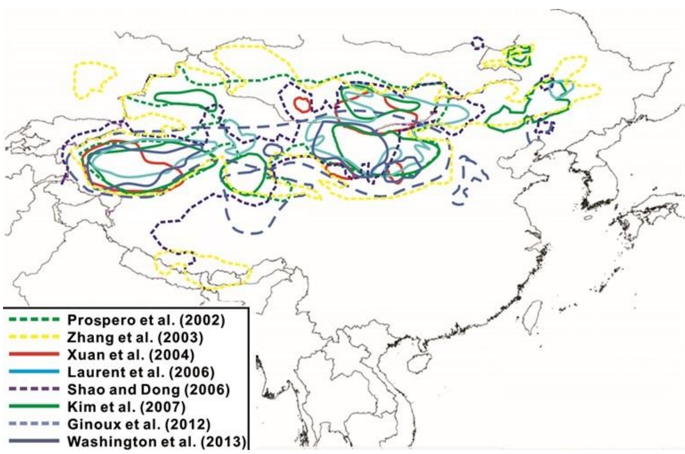

Figure 4. Review of potential source areas over East Asia in the published literature (updated from Formenti et al., 2011b)

An inter-comparison between our results and other available data on dust sources revealed that the southwestern area of Mongolia and its neighboring region in China, the northeastern area of Mongolia and the central part of Northeast China are also significant sources of dust emissions. It is particularly notable that aeolian emissions from these regions can readily lead to long-range transported dust storms. For example, the dust events 27, 79 and 117 formed in Mongolia and were transported via Northeast China by the Mongolian cyclone and Arctic Oscillation (Takemi and Seino, 2005; Dickerson et al., 2007; Mao et al., 2011), and even reached the Russian Far East region (Kondratiev and Skalyga, 2011) (Figure 6b of this study).

Unlike African source regions, East Asia is a complex and inhomogeneous dust production area with different types of single sources (e.g. desert, Gobi, grassland, cropland) presenting distinct properties such as soil texture, mineralogical composition, aggregation and crusting. These all affect the source strength. Xuan et al. (2004) defined the Asian dust source region as two parts or systems: the Mongolian Plateau and the Tarim Basin. However, this classification may be too coarse geographically. The erodibility map established by Ginoux et al. (2012) and the dust source map complied by Prospero et al. (2002) revealed the general distribution of dust emission areas across the world. Here, we further reviewed previous studies and compiled the distribution of dust sources over East Asia (see Figure 4) based on the study of Formenti et al. (2011b). It is obvious that the Taklimakan desert and the arid areas which cover central northern China and central southern Mongolia are major dust sources. However, the distributions of dust sources in other areas (e.g. Northeastern China) are different from one another according to previous studies, which would significantly affect the dust prediction on a sub-regional scale.

Atmos. Chem. Phys. Discuss., doi:10.5194/acp-2016-681, 2016
Manuscript under review for journal Atmos. Chem. Phys.
Published: 10 October 2016

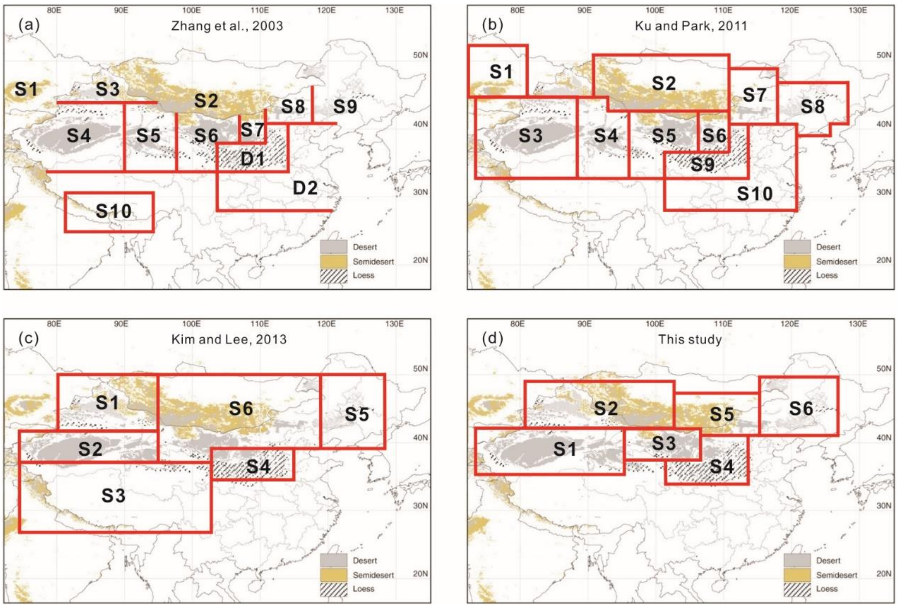

Figure 5. Comparison of our optimized division of dust source regions with previous partition schemes in regional dust modeling over East Asia.

In order to effectively characterize the sub-regional features and simplify modeling comparisons, different division schemes adopted in former studies are depicted in Figure 5a, 5b and 5c (Zhang et al., 2003; Ku and Park, 2011; Kim and Lee, 2013). According to the MODIS image series, we further subdivided the dust emission sources into six distinguishable sub-regions according to their regional characteristics and frequency of dust events (Figure 5d). Among the 214 dust events in China and Mongolia identified by MODIS, most originated in regions S1, S3 and S5 (Table 1 in the supplemental information; Figure 5d). The three main sources (Taklimakan Desert, Gobi, sandy lands in Region 1), in terms of numbers of dust events, accounted for over three quarters of the total dust emission events in East Asia, in contrast to the results of Zhang et al. (2008). Propelled by cold frontal systems and the Mongolian cyclone, dust from the five regions generally moves eastward, but with some regional differences in transported direction (Figure 6a).

3.2.1 Region 1

The Region 1 sources mainly cover the Taklimakan, Gurbantunggut and Kumtag

Deserts, Hashun gobi-desert, Turpan-Hami Basin (gobi-desert) and Qaidam Basin (gobi-desert and playa). MODIS data showed that the Taklimakan desert was an important long-distance transport and local dust source throughout the year, except for the summer. The main local dust source was located along the northeastern rim of the Tarim Basin, where dry river beds and salt lakes lie between the desert and alluvial fans (Washington et al., 2003). However, the suspended dust was always transported along the edge of the basin from northeast to southwest, partially along the Hexi Corridor (Gao and Washington, 2010). As the entry of cold air masses is blocked by the high elevation and the dust-laden atmosphere is poorly ventilated, most local dust events originating in the Taklimakan desert are not easily transported out of the Tarim Basin, and instead are mainly deposited on the windward slopes of the Kunlun Mountains (which could be verified by AOD distribution in Figure 9).

The Taklimakan Desert's role as a strong dust emission source has been identified by frequency statistics (Kurosaki et al., 2003), numerical modeling (Laurent et al., 2005; Tanaka et al., 2006; Wang et al., 2008) and satellite monitoring (Engelstaedter and Washington, 2007; Gao and Washington, 2010; Waggoner and Sokolik, 2010). Once the dust is uplifted by strong winds to elevations exceeding 5000 meters, the dust may be transported eastward, climbing over the Hexi Corridor to begin its long-distance transport over East Asia, even reaching North America and Greenland (Uno et al., 2009).

Xuan et al. (2004) suggested that the Taklimakan desert and the Tibetan Plateau are active dust sources only in the late spring and early summer, because the solid frozen crust prevents dust emission. Our results show that the first dust event over the Taklimakan desert was detected in late winter and early spring. It is likely that the surface of the intensely arid desert does not form a solid crust when frozen.

3.2.2 Region 2

Region 2 sources include the Junggar Basin with the Gurbantunggut Desert, the Great Lakes Basin in western Mongolia and Gobi Desert in southwestern Mongolia covering three provinces—Bayankhongor, Govi-Altai and Zavkhan. The Aibi Lake region, Gurbatunggut Desert and agricultural development region in Kelamayi are three major sources for dust emission (Qian et al., 2007). The southeastern side of the Altay

Mountains and the Central Gobi-desert together form one of the most frequent dust sources in Mongolia (Tsolmon et al., 2008). Previous studies have shown that the maximum dust emission rates occur in Outer Govi-Altai, in the same place as the maximum aridity, and the greatest occurrence of dusty days occurred in the Gobi Desert and the Great Lakes hollow of west Mongolia (Natsagdorj et al., 2003; Xuan et al., 2004). MODIS monitoring showed that this region was the source of more than 19% of the dust events originating in East Asia.

3.2.3 Region 3

Region 3 sources include the Gobi and sandy deserts in the Hexi Corridor, and the Alxa Plateau (including Badain Juran Desert, Tengger Desert and Ulan Buh Desert in north-central China). Guaizihu and Minqin have been reported as the two major dust storm centers in the Alxa Plateau based on observational data from meteorological stations from 1961 to 2005 (Yao et al., 2011). Variability of the climate has had less impact on aeolian desertified land expansion than that of human activities over this region (Wang et al., 2013).

MODIS observations during 2000-2015 showed that this region accounted for about 30% of the total number of dust events. Many “hot spots” or “dust plumes” along the China-Mongolia corridor were important point-source contributors to dust emissions from this region during 2000 - 2013. These point sources mainly comprised dry lakes, river beds and alluvial fans. Juyan Lake and Guaizihu were the two areas with the most frequent dust emissions in this region.

3.2.4 Region 4

Region 4 sources mainly comprise the Qubqi Desert, Mu Us Sandy Land on the Ordos Plateau and the Loess Plateau. The Loess Plateau is a potential dust emission source because its surface soil consists of fine silt and clay particulates. However, our observations revealed the low frequency of dust storm occurrences on the Loess Plateau (5 dust events), except in its northwest part in Gansu province and Ningxia Hui autonomous region which are adjacent to the regional deserts. Xuan et al. (2004) also found that the vast area of the Loess Plateau was not a strong dust source when compared to other regions, due to the high clay content in the surface soil.

Atmos. Chem. Phys. Discuss., doi:10.5194/acp-2016-681, 2016
Manuscript under review for journal Atmos. Chem. Phys.
Published: 10 October 2016

Atmospheric Chemistry and Physics Discussions
Open Access

3.2.5 Region 5

Region 5 sources mainly include the Gobi Desert around Ulaan-nuur Lake in Central-Eastern Mongolia, the Gobi Desert around Dornogov province of Southeastern Mongolia (which includes the Doolodyn Gobi-desert, the Ooshiyn Gobi-desert and Dalay-Els Sandy Land) and the Otingdag Sandy Land of China.

MODIS monitoring shows that this region is the principal contributor (42%) to long-range dust transport to the North Pacific. Dust from Region 5 can follow two main transport pathways (Figure 6a): eastward, rising over the Da Xinganling mountain ranges, to the North Pacific; or southeastward, climbing over Yishan Mountain and Taihang Mountain, over the Bohai Sea, and then across the Korean Peninsula to the Sea of Japan and beyond.

3.2.6 Region 6

Region 6 sources are mainly made of the Horqin Sandy Land, the saline and alkaline land around the northeast China plains, the Hunlun Buir desert, and the Moltsog-Els and Ongon-Els sandy lands of eastern Mongolia. In this region, there are also dozens of small sources associated with pasture, dry lakes, river beds, or alluvial fans.

Compared to dust source divisions adopted in three former studies (Figure 5), the dust source area around Lake Balkhash should be excluded from the East Asia region and reassigned to Central Asia (Xin et al., 2015). The role of the Tibetan Plateau has become controversial and will be further discussed in section 3.3. The central part of eastern China (D2 in Figure 5a), which is mainly composed of dry cropland with irrigation, was also excluded as a major dust source in this study, and wind erosion over this region needs further detailed study. Besides the regular eastward (to Korea and Japan) and southeastward (to Taiwan and Hong Kong) transport routes, our trajectory analysis also shows that the dust could even been transported directly northward to the Far East region by the Mongolia cyclone. Two former studies have demonstrated that the dust emitted from East Asia could reach the Arctic Circle via the Japan Sea (Cahill, 2003; Huang et al., 2015). The transported dust potentially affects the climate and ecosystem of the Arctic region, thereby complicating the process of climate change in the Arctic (Di Pierro et al., 2011).

Atmos. Chem. Phys. Discuss., doi:10.5194/acp-2016-681, 2016
Manuscript under review for journal Atmos. Chem. Phys.
Published: 10 October 2016

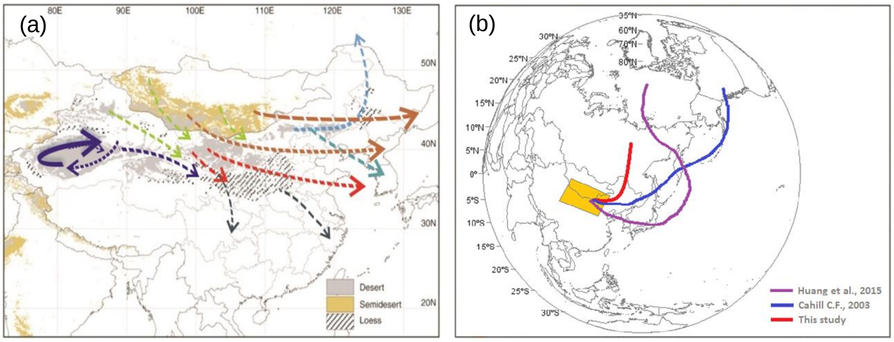

Figure 6. Dust sources and transport pathways identified by MODIS and HYSPLIT model. (a) The purple solid arrow indicates the uplift of transported dust. (b) Three major trajectories of transported dust reaching the Arctic.

3.3 Hotspots of dust emission on a sub-regional scale

The main aim of this section is to detect the dust source hotspots by means of the MODIS images. In some instances, dust plumes may be discernible in the MODIS VIS (e.g. Figure 7); but this was certainly not always the case. Average AOD values over long time series have been used to detect persistent, regional scale dust sources (e.g. Ginoux et al., 2012) but accurate and event-specific source identification requires the clear delineation of the upwind margin of the plumes. Rather than being sourced from large homogeneous areas, much of the global supply of dust comes from hotspots, which are small but relatively consistently active dust-producing areas (Gillette, 1999). Hotspots in the form of dry lakes, river beds, alluvial fans, mines, and croplands can contribute to dust emissions in the arid and semi-arid areas of Africa and Asia (Bullard et al., 2008; Zhang et al., 2015a). Identification of hot spots within the huge areas identified as sources of dust on a regional scale is necessary to improve numerical modeling of dust emission and transportation, to develop effective countermeasures to hinder wind erosion, and to allow precautions to be taken against dust-related health problems.

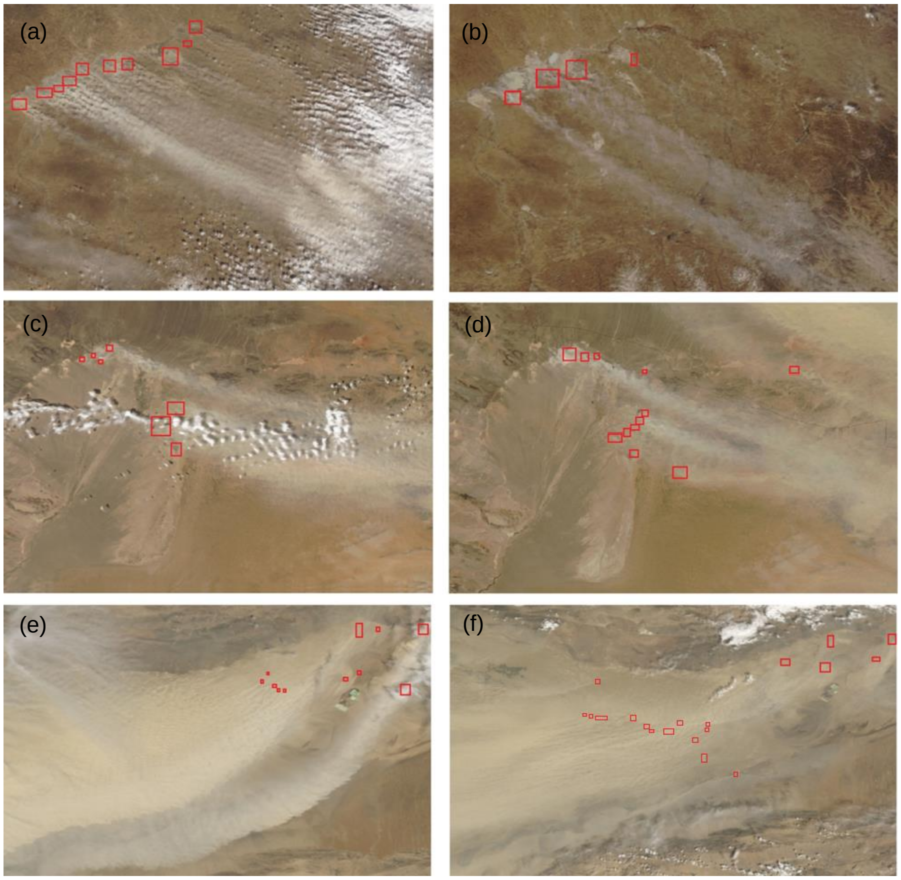

Figure 7. Across all panels: squares highlight the prominent active dust hotspots with obvious dust plumes, as identified in the BTD split window product. (a) and (b) : Ulgai Gaobi in Northeastern China; (c) and (d): Juyan and Guaizi Lakes in the Gobi alluvium area; (e) and (f): Lop Nur in the Tarim Basin

Dust production occurs in hotspots at scales of the order of 1-10 km or less, with each hotspot producing a "point source plume". High-resolution satellite imagery and field data show how numerous point source plumes merge to form regional and synoptic scale dust plumes. Hence we suggest that a thorough understanding of the life cycle of these point source plumes, obtained via numerical modeling, is vital for the accurate parameterization of coarse resolution dust plumes in synoptic and global scale models. (Walker et al., 2009).

Areas satisfying the following three criteria are classified as hotspots in this study. (1)

Lowest threshold wind speed and without snow and/or vegetation cover. (2) Land use type promotes dust emission, for example lake and river beds, alluvial fans, and bare cropland. (3) An area with the highest dust emission frequency and magnitude.

Individual or multiple simultaneously active hotspots can be distinguished within the satellite images at the beginning of dust plumes. Based on the identified 214 dust storm events in this study, we also investigated the spatial-temporal distribution and inventory of hotspots over East Asia. Four major regions with several hotspots were discriminated, these were regions S1, S3, S5 and S6 shown Figure 5d.

By analyzing more than 1326 MODIS images, we identified hotspots scattered across the dust source region of East Asia and considered their potential for dust emission on the basis of their land cover. Table 3 summarizes the most viable hotspots and the erodibility features with which they are likely to be associated as inferred from Google Earth, Global Mosaics of the standard MODIS land cover type data product (MCD12Q1) of China and Mongolia (http://glcf.umd.edu/data/lc/, Channan et al., 2014) and visual field observations. Of these sources, the majority (eighteen) feature dry lakebeds and paleolakes or bare riverbeds and paleochannels; seven feature outwash fans over steep hillsides; and three hotspot sub-regions feature barren sandy land or saline and alkaline land. Note that with the exception of the highlighted sources in Table 3, it is also important that seasonally bare cropland regions (e.g. Northeast China Plain and North China Plain) can contribute, albeit infrequently and weakly, as sources of dust storms. Winds in excess of the thresholds needed to start saltation are presumably exceeded in these areas, but these threshold winds do not evidently occur frequently and there is a limited time when surface soil is free from vegetation and prone to wind erosion (Zhang et al., 2015a).

Due to the significant differences in threshold wind speed and vegetation index between Gobi and sandy lands (Laurent et al., 2005), our results show that hotspots in the Gobi appear to be larger than those in the sandy lands, and dust emissions were more intense over these hotspots (Figure 7).

Atmos. Chem. Phys. Discuss., doi:10.5194/acp-2016-681, 2016
Manuscript under review for journal Atmos. Chem. Phys.
Published: 10 October 2016

541 Table 3. Details of 24 identified hotspots for dust emission with erodibility features over East Asia, based on MODIS data, during 2000-2015.

Label	Position	Named Features or Position Description	Erodibility Features	Regions*
A	40.5-41.0°N, 91.0-91.5°E	Northeastern corner of Turfan depression	Bare desert	1
B	40.3-40.7°N, 90.0-91.7°E	Northeastern corner of Turfan depression	Paleochannels	1
C	40.5-40.8°N, 88.8-89.3°E	Northeastern rim of Taklimakan desert	Paleochannels with diffuse sand	1
D	40.6-41.0°N, 83.8-84.8°E	Central northern rim of Taklimakan desert	Paleochannels	1
E	36.0-37.6°N, 80.6-90.3°E	Southeastern rim of Taklimakan desert	Outwash fans	1
F	37.4-38.8°N, 89.2-94.1°E	Northern part of Qaidam basin	Outwash fans over steep hillside,	1
G	39.3-40.6°N, 93.8-97.0°E	Western part of Hexi corridor	Outwash fans, paleochannels	1
H	42.7-43.3°N, 89.3-94.0°E	Eastern Mt. Tianshan	Outwash fans over steep hillside	2
I	44.9-45.1°N,101.8-102.3°E	Western central part of Uvurkhangai of Mongolia	Sand dunes, river beds and lake	2
J	44.4-45.6°N, 99.3-101.3°E	Central part (Oroi Nuur Lake)	Lake beds, Mountain valley	2
K	42.8°N,103.0°E;	Central part of Umnugovi, Mongolia	Mountain valley, paleolakes and	2
L	46.6-47.3°N,107.5-110.5°E	Southwestern part of Tov	Paleolakes, river beds	2
M	45.6-45.8°N, 85.1-85.5°E	Western part (Sayram Lake) of Junggar basin	Saline and alkaline land, lake beds	2
N	43.0-44.8°N, 92.2-95.6°E	Eastern part (Barkol Lake) of Jungger basin	Outwash Plain, paleochannels,	2
O	41.5-42.5°N,100.5-102.0°E	Juyan Lake in Ejin Banner of Inner Mongolia	Rim of huge outwash fan with lake	3
P	41.3-42.6°N,104.5-105.0°E	Northern part of Alxa Left Banner, Inner Mongolia	Paleolakes	3
Q	42.3-42.7°N, 97.9-99.3°E	Northwestern part of Ejin Banner, Inner Mongolia	Paleolakes	3
R	38.7-39.1°N,101.6-102.7°E	Eastern part of Hexi corridor	Outwash fans over steep hillside	3
S	39.1-39.3°N,108.2-109.5°E	Central part of Mu US sandy land	Lake beds	4
T	43.1-43.7°N,112.9-115.4°E	Southern part of Otingtag sandy land (Hunshandake)	Paleolakes, lake beds and river	5
U	44.2-45.3°N,110.0-111.7°E	Central eastern part of Dornogovi of Mongolia	Lake beds and nearby outwash	5
V	42.5-43.3°N,110.6-111.8°E	Central part of Sunitezuo banner, Inner Mongolia	Paleochannels, sandy land	5
W	45.4-45.7°N,117.3-118.7°E	Ulgai Gaobi in Ujimqin Banner of Inner Mongolia	Lake beds	6
X	42.8-45.3°N,118.3-122.3°E	Southeastern part of Inner Mongolia	River beds, lake beds, sandy land,	6

542 * Index of typical events with identified dust plumes are listed in Sheet 2 of the appendix.

Atmos. Chem. Phys. Discuss., doi:10.5194/acp-2016-681, 2016
Manuscript under review for journal Atmos. Chem. Phys.
Published: 10 October 2016

Atmospheric Chemistry and Physics
Open Access
Discussions

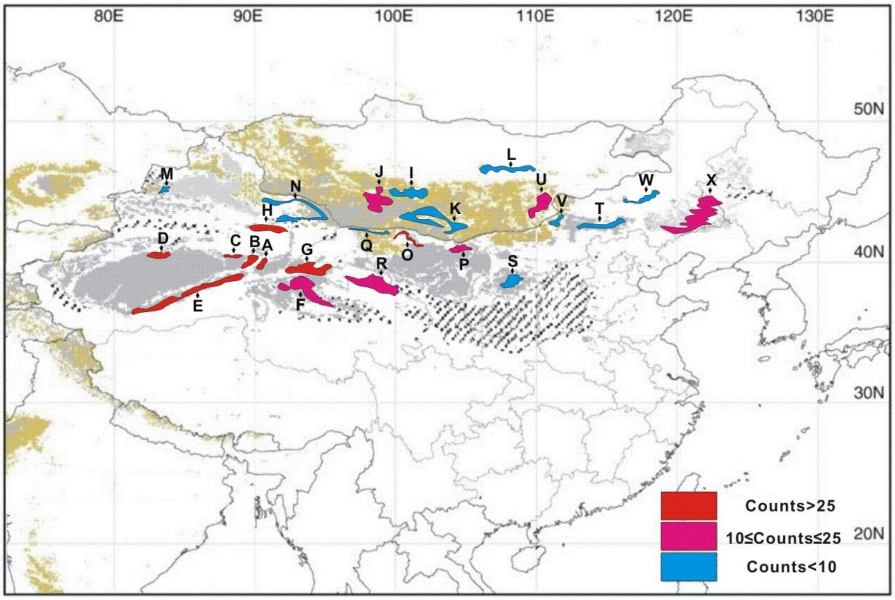

Figure 8. Spatial distribution of 24 identified hotspots with labels from Table 3 along with their dust event counts, in East Asia (Grey shades represent deserts, yellow shades represent semi-deserts and the stripped lines represent the distribution of losses).

The spatial distribution of 24 identified hotspots along with dust event counts is illustrated in Figure 8. It is obvious that the high-frequency hotspots are located in western China, and the medium-frequency hotspots are located in southern Mongolia and northeastern China. This spatial distribution of dust hotspots is also consistent with the spatial variation of dust events based on ground observations in former studies (see Section 3.1). In order to verify the accuracy and further understand the regional effects of these 24 hotspots, we next mapped the average deep blue AOD at 550 nm over terrestrial East Asia from March 2000 to October 2015 (Figure 9). Besides the two well-known heavy air pollution areas (the southern rim of the Tibetan Plateau, covered with brown cloud; and eastern China, covered with haze), half of the hotspots could be distinguished at the regional scale with a resolution of 1° × 1°. This implies that the significant contribution of dust hotspots to regional air quality cannot be neglected. However, while higher AOD values were observed across the northern and central Tibetan Plateau (white dashed rectangle in Figure 9), no obvious hotspots were identified over the Tibetan Plateau. This could be because dust is uplifted and transported from the southern rim of the Qaidam basin under the prevailing winds, subsequently becoming dispersed across the Tibetan plateau because of the 'elevated heat pump' effect as indicated by 3-D satellite observations of aerosol over this region coupled with the assistance of CALIPSO (Gao and Washington, 2010; Jia et al., 2015; Xu et al., 2015). Thus, we concluded that the Tibetan plateau is a receptor region of transported dust but not a significant dust emission source area in East Asia. Higher AOD values were also observed in central northern China (blue dashed rectangle in Figure 9), owing to the anthropological aerosol emissions from city groups in oases within the arid region. The anthropogenically related, high AOD values under the blue dash-dot lines over Northern Indian subcontinent and Eastern China are also represented in Figure 9.

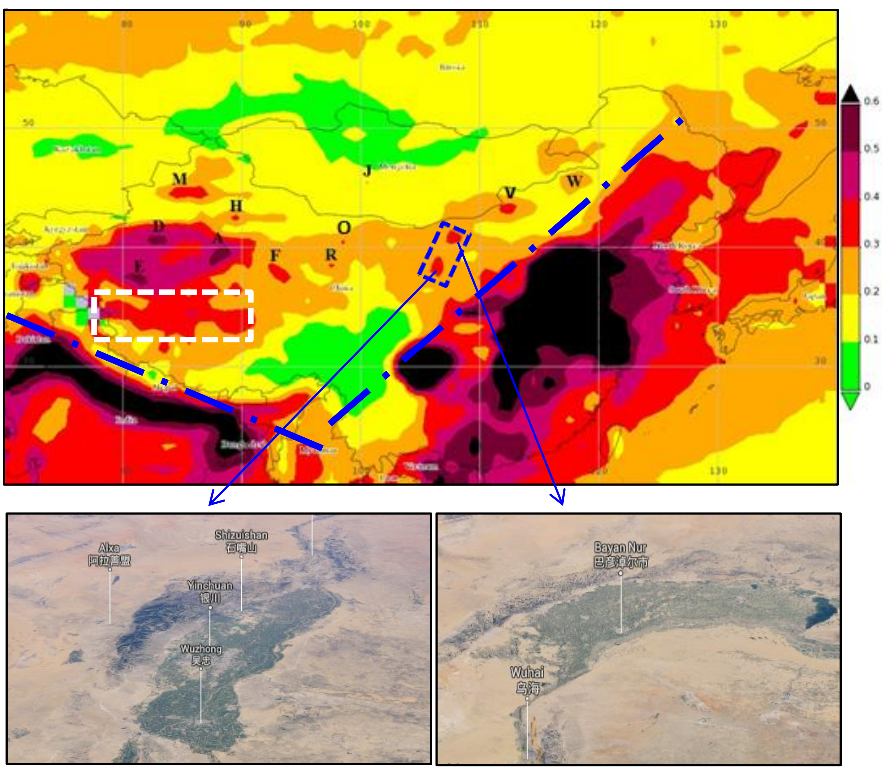

Figure 9. Time-averaged map of deep blue aerosol optical depth at 0.55 um over East Asia from March 2000 to December 2015 (Bold letter labels corresponded to the identified hotspots in Figure 8; the

Atmos. Chem. Phys. Discuss., doi:10.5194/acp-2016-681, 2016
Manuscript under review for journal Atmos. Chem. Phys.
Published: 10 October 2016

Atmospheric Chemistry and Physics
Open Access
Discussions

subpanels showed the city groups located in oases with central coordinates of 40.9° N, 107.6° E and 38.7° N, 106.3° E).

The three most important areas, containing several hotspots, are described in more detail in this section. The most frequent hotspots are located at the northeastern corner of the Tarim Basin, precisely over Lop Nur centered at ~90° E, 40° N. The surrounding mountains act as barriers which complicate the circulation pattern over the basin. Lop Nur was a large saline lake (~2000 km^2) in the 1930s which dried up in 1962 (Li et al., 2008). Water diversion projects on the Tarim River, which drains the Tarim Basin, reduced the inflow to such a degree that the lake is now a dry salt lake, largely salt-encrusted and subject to severe wind erosion. Interestingly, the frequency of dust plumes has obviously increased over this region (Label **A**, **B** and **C**) since 2010. Meanwhile, a dramatic expansion of brine-evaporation pools occurred: from 25 km^2 before 2009 to 180 km^2 after 2010. Furthermore, an extensive network of artificial canals with a total length of 145 km was excavated to collect infiltrated brine, which would further accelerate the loss of surface water and development of drought in Lop Nur (Figure 10). However, a more detailed mechanism linking the development of saline lakes and increased dust events over Lop Nur needs to be further investigated in our future works.

Figure 10. Historical MODIS images showing the development of a saline lake factory with marked artificial canals for infiltrated brine in Lop Nur, Taklimakan desert.

Atmos. Chem. Phys. Discuss., doi:10.5194/acp-2016-681, 2016
Manuscript under review for journal Atmos. Chem. Phys.
Published: 10 October 2016

Atmospheric Chemistry and Physics
Open Access
Discussions

Another dust emission hotspot region is the western Gobi alluvium area (Label **O** in Table 3) of the Alashan Plateau, along with dust hotspots distributed along the dried lake beds of Juyan and Guaizi Lakes (Figure 7c and 7d). The Juyan Lakes consist of West Juyan Lake (Gaxun Nur) (42.5° N, 100.7° E) and East Juyan Lake (Sogu Nur) (42.3° N, 101° E) at the terminus of the Hei River originating from the north flank of the Qilian Mountains. These lakes dried up in 1961 and in 1994. In these potential emission areas, contrary to expectation, the soils are not sandy desert but instead are semi-lithified deposits of fine-grained mud/silt substrates, according to remote sensing analysis with field validation (Wang et al., 2004; Figure 3 in Yang et al., 2008 and Figure 11d in Taramelli et al., 2012). Protecting grasslands in the lower reaches of the river basin from degradation and rehabilitating the dried-up terminal lake would be highly beneficial in reducing dust plumes in the region.

The third focused area comprises the dried lake beds of the Wulagai Lake group and barren grass or vegetated lands in the Otindag Sandy Land (Label **W** in Table 3 and Figure 7a and 7b). In this grassland area, coal mining industries had caused rapid shrinkage and even drying up of the Wulagai Lake group by 2004 (Tao et al., 2015).

The fourth area is distributed over the Horqin sandy land and the saline soils in western Jilin Provence (Label **X** in Table 3). According to the positions of the origins of dust plumes identified in this study, hotspots contributed much to the dusty weather experienced over Northeastern China, and the dust was transported to Korea, Japan and even to far eastern Russia.

An additional two dry lake beds in Mongolia, at Boon Tsagaan Nuur (45.6° N, 99.1° E) and Oroi Nuur (45.1° N, 100.7° E), were also identified as dust hotspots. The central part of Mongolia (Labels **I**, **K**, **L** and **U**) is fed by fine-grained material from alluvial fans and ephemeral steams and is therefore highly susceptible to wind erosion.

The use of protective farming techniques, afforestation and water conservation in dust emitting basins, along with dust suppression and protection of water resources in mining areas, should be considered to combat dust emissions in the hot spot areas identified in this study.

4. Implications for dust modeling and forecasting

The above discussion revealed that East Asia is a complex, inhomogeneous dust production region comprising various types of individual sources, each having distinct properties and different strengths. Dust models combine dust source information with predictions of atmospheric dynamics to forecast the occurrence of dust events. The key component of a dust forecast model is its treatment of dust sources and emissions, however, heterogeneous dust source maps are presented in different models in East Asia (Figure 11). If the dust source map is inaccurate or ambiguous, the emission flux and spatial-temporal distribution of the modeled regional dust distribution will be erroneous. The fact that global dust emissions are controlled by a few very productive sources provides useful information to design efficient mitigation strategies (Engelstaedter and Washington, 2007; Haustein et al., 2015). The concept of preferential dust sources (Ginoux et al., 2001; Bullard et al., 2011) acts to nudge models towards the observed dust emission patterns by relaxing the threshold emissions and, in essence, removes the surface crusting issue from the modeling process. Nevertheless, none of the current model emission schemes is able to reproduce the spatial distribution of the major dust sources correctly (Haustein et al., 2015).

Traditionally, models have used the bare ground categories of land cover maps to locate dust sources. However, new model representations of dust sources are based on topographic, hydrologic, and geomorphologic considerations; alternatively they are derived directly from satellite data, for example considering the surface bareness, topographical depression features and soil freezing and thawing. The latter approach includes surface reflectance, frequency of high aerosol values, and ultraviolet-visible albedos. Waggoner and Sokolik (2010) suggested that soil with a high silt-to-clay differential or ratio will have a higher albedo and act as a preferential source for potential dust emission. These new representations provide a much more refined view of global and regional dust source regions.

Table 4. Comparisons of dust source functions/maps in different dust numerical models covering East Asia

Model or Satellite	Region 1	Region 2	Region 3	Region 4	Region 5	Region 6	Reference
TOMS AI	√		√				Prospero et al., 2002
TOMS AI	√		√	√			Engelstaedter and Washington, 2007
TOMS AI	√	√					Varga, 2012
MODIS AOD	√	√ +**UCM**	√	√	√ +**UCM**	√ + **LHN**	Ginoux et al., 2012
GOCART	√ + **LTB**		√	√			Ginoux et al., 2001
HYSPLIT[#]	√		√	√		√ + **LSL**	Draxler et al., 2010
NMMB/BSC	√		√				Pérez et al., 2011
CFORS	√ + **OTP**	√	√	√ + **LLP**			Uno et al., 2006
MASINGAR	√		√ + **LNM**	√ + **LLP**		√ + **LHL**	Tanaka et al., 2006
ADAM			√	√	√ + **OWR**	√ + **OWR**	Park and In, 2003
ADAM2	√ + **OTP**	√	√	√	√	√	Park et al., 2010
CUACE/dust	√	√ + **LNM**	√	√ + **LLP**	√	√ + **LSL**	Gong et al., 2003
TAQM/dust	√	√ + **LNM**	√	√	√	√ + **LSL**	Tsai et al., 2008
WRF-Chem	√	√ + **LNM**	√	√	√	√ + **LSL**	Kang, 2011

[#] https://ready.arl.noaa.gov/documents/Tutorial/dust/dust_global.zip; **UCM**: Underestimation of the central part of Mongolia; **LTB**: Lack of the Tarim Basin; **LNM**: Lack of the northern part of Mongolia; **LTD**: Lack of the Tengger desert; **LLP**: Lack of the Loess Plateau**;** **LHL**: Lack of the Hulunber sandy land; **LHN:** Lack of the Hunshandak sandy land **OTP**: Overestimation of the Tibetan Plateau; **LSL**: Lack of salty-kaline land in Northeastern China

In this section, we compared the dust source maps for mesoscale and global-scale dust models which cover the region of East Asia in Table 4 and Figure 11. This demonstrates that source maps in most of the numerical dust models are deficient relative to the identified regions in this study; only the ADAM2 model has a comparative distribution but this model overestimates dust over the Tibetan Plateau.

More recently, instead of employing a fixed source map, some researchers have adopted a dynamic dust source allocation. For example, a dust source function (or probability of dust uplifting with a value between 0 and 1) is defined as the product of the topographical depression and surface bareness in the GOCART model (Ginoux et al., 2001), while the land cover change and seasonal variations of soil bareness have been considered by incorporating the dynamic NDVI from satellite observations (Kim et al., 2013). Kok et al. (2014) developed a new physical dust emission scheme that does not require a dust source map but depends dynamically on the soil bareness (linearly related to the leaf area index) and soil texture (clay fraction). Zhang et al. (2015c) related the wind friction in physical dust emissions to land use and soil texture data without predefining a static dust source map, and thus enabling the modeling of wind erosion over croplands.

Atmos. Chem. Phys. Discuss., doi:10.5194/acp-2016-681, 2016
Manuscript under review for journal Atmos. Chem. Phys.
Published: 10 October 2016

Atmospheric Chemistry and Physics
Open Access
Discussions

As mentioned above, we divided the dust source functions/maps presented earlier into eight categories: 1) topography (Ginoux et al., 2001); 2) topography combined with soil bareness (Kim et al., 2013); 3) surface roughness (Laurent et al., 2005; Koven and Fung, 2008); 4) geomorphological classification (Bullard et al., 2011); 5) back-tracking by satellite observation (Schepanski et al., 2009); 6) a threshold-frequency method using ground or satellite observations (Park et al., 2010; Schepanski et al., 2012); 7) the self-organizing map (SOM) neural network method (Lory et al., 2016); and 8) a dynamic physical-mechanism method (Kok et al., 2014; Zhang et al., 2015c). However, more detailed inter-comparisons between the above eight methods need to be conducted over the East Asia region in future works to improve the modeling and forecasting of dust events, in particular the weak, small-scale dust emissions.

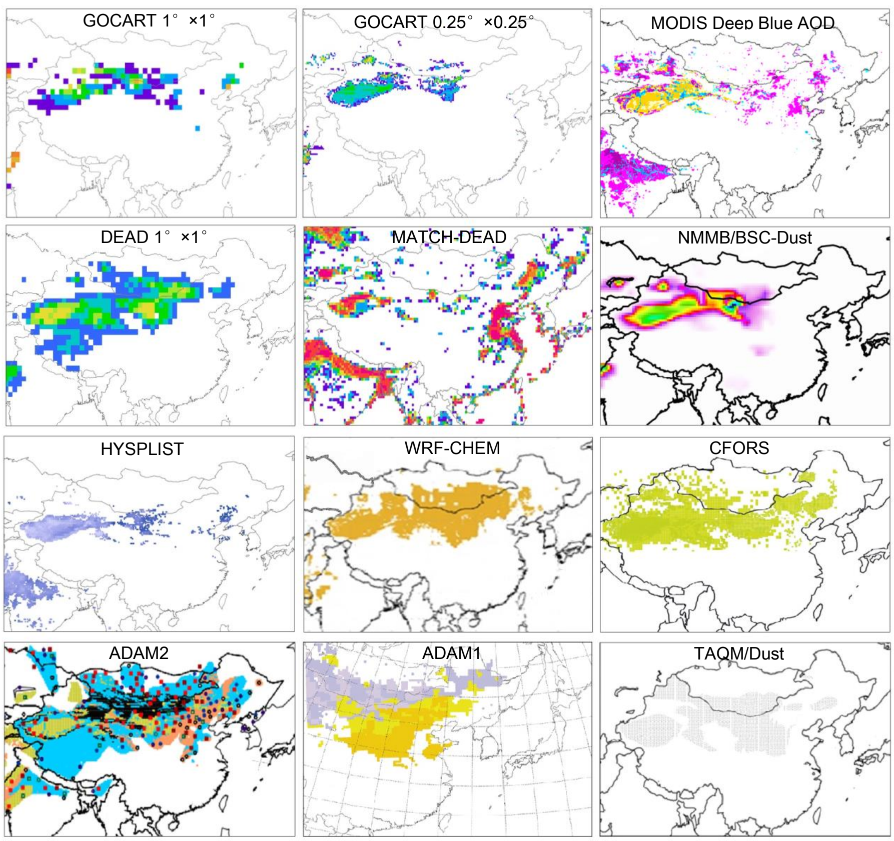

Figure 11. Comparison of the spatial distribution of preferential dust source maps/functions in 12 dust

numerical models covering East Asia

Bullard et al. (2011) developed a simple classification of geomorphic types related to their behavior as dust sources, based on current understanding of the geomorphological controls on dust emissions. The authors also pointed that this scheme can be applied to map potential modern-day dust sources in four major dust source regions (the Chihuahuan Desert, the Lake Eyre Basin, the western Sahara and the Taklimakan), primarily using remote-sensing imagery to classify surfaces, and thus is suitable for global application. However, while detailed geomorphological mapping has been achieved for some regions, at present there is no standardized methodology or dataset for global scale coverage. Furthermore, the method has only been specifically validated for the Chihuahuan Desert in North America and the Lake Eyre Basin in Australia (Bullard et al., 2011; Baddock et al., 2016). Comparing plots of dust sources over the Taklimakan in Figure 2 of Bullard et al. (2011) with Figures 8 and 9 in this paper, we observe that the geomorphological method performs poorly over East Asia and needs further careful validation.

As mentioned in Section 3.1, the frequency of dust events can increase in other seasons besides the spring, and thus the regional dust storm forecasting system should be operational for the whole year rather than intermittently (for example, the Asian dust forecasts from the Korea Meteorological Administration are only provided from March to May (http://web.kma.go.kr/eng/weather/asiandust/forecastchart.jsp). Based on demands for forecasting hazards related to poor air quality, traffic visibility and resident health, a framework for sub-regional forecasting of the onset and development of dust plumes and their effects on downwind regions should be urgently established in local meteorological organizations, especially in the regions containing several of the hotspots identified in Table 3.

5. Conclusions

In this paper, the use of MODIS products has achieved significant improvements in quantifying atmospheric dust: first in the assessment of the temporal variability of dust events, and then in identifying dust sources and hotspots for the period 2000-2015. The combined use of MODIS L1B data and the BTD algorithm provided an effective method of dust discrimination and hotspot validation. Furthermore, the dust emission source locations were divided into six distinct sub-regions according to their geographical characteristics and frequency of dust events, thereby aiding future regional modeling studies. Comparing dust source maps and functions in current dust models with those applied to the whole East Asia has also revealed that heterogeneous distribution of dust sources is still one of the major factors that affects the prediction accuracy of dust events in East Asia.

Having systematically analysed the satellite data, we highlight the following key findings and implications.

1) A relatively detailed inventory of dust events in East Asia during the past 16 years has been established based on satellite observations. A slightly increasing tendency was observed during the study period; however, the seasonal variability was significant, and the frequency of dust events in spring sharply decreased while the frequency slightly increased in summer and autumn.
2) It is clear that the Tibetan Plateau is not an important dust source region in East Asia, and the contribution of this region has been overestimated in some previous studies. Meanwhile, northeast China, one of the major dust sources, has been overlooked or underestimated by most previous modeling studies, yet dust from this region can be transported to the Far East. Besides the regular eastward (to Korea and Japan) and southeastward trajectories (to Taiwan and Hong Kong), our trajectory analysis has also shown that the dust can even be transported northwards to the Far East region by the Mongolia cyclone. The transported dust potentially affects the climate and ecosystems of the Arctic region, therefore complicating the impact of climate change in the Arctic.
3) Twenty-four dust hotspots were identified in East Asia, of which the high-frequency hotspots were located in western China, and the medium-frequency hotspots were located over southern Mongolia and northeastern China. Anthropogenic activities appear to be the dominant causes of dust emissions from the medium-frequency

hotspots. Further studies need to develop our understanding of the relationships between small-scale changes in land cover, population and industrial growth, and changes in the redistribution of hot spots. The hotspots identified on the basis of MODIS L1B data provide small-scale information about dust emissions and can be used to improve both our understanding of regional- to global-scale dust cycles and numerical modeling of dust emission and transport.

4) Current dust models commonly use semi-empirical dust source functions to help parameterize spatial variability of dust emissions. A high-resolution (1 km) dust source database for East Asia is still lacking. The dynamic, physically-based approach used in dust models reduces the need to use an empirical source function in global dust cycle simulations; however, down-scaling this scheme to the mesoscale needs to be further verified. This also emphasizes the importance of reliable and higher resolution soil texture data.

There is still work to do with respect to establishing high-resolution gridded datasets of the dust sources and hotspots identified in this study, and the real test of our findings will only come when these data are implemented and compared with other predefined sources within a dust-cycle model. In this context, we note that the human activities, especially the unreasonable exploitation of water resources, are another key factor which may cause dry lake beds to become dust hotspots and exacerbate the regional dust emissions. We will quantify this human contribution to regional dust emission and climate forcing in a forthcoming study using a regional climate model.

Acknowledgement

This research was funded by NSFC (Grant No. 41571063, 41205108 and 21407148). The project was also supported by the Open Research Fund of Key Laboratory of Tibetan Environmental Changes and Land Surface Processes, Chinese Academy of Sciences (Grant No. TEL201504). We thank the National Snow and Ice Data Center (NSIDC) and the Level 1 and Atmosphere Archive and Distribution System (LAADS) for the provision of satellite data. The authors gratefully acknowledge the NOAA Air Resources Laboratory (ARL) for providing the HYSPLIT transport and dispersion model used in this publication.

Atmos. Chem. Phys. Discuss., doi:10.5194/acp-2016-681, 2016
Manuscript under review for journal Atmos. Chem. Phys.
Published: 10 October 2016

The authors would like to thank Drs. Mo Dan and Weiwei Chen for their technical assistance and useful discussions.

References

Ackerman, S. A.: Remote sensing aerosols using satellite infrared observations, J. Geophys. Res.-Atmos., 102, 17069-17079, 1997.

Anderson B. A., and Brode, R. W.: Evaluation of four lagrangian models against the Cross-Appalachian and European Tracer Experiments, 2010 EPA modeling workshop, Portland, Oregon, 2010.

Ashpole, I. and Washington, R.: A new high-resolution central and western Saharan summertime dust source map from automated satellite dust plume tracking, J. Geophys. Res.-Atmos., 118, 6981-6995, 2013.

Atkinson, J. D., Murray, B. J., Woodhouse, M. T., Whale, T. F., Baustian, K. J., Carslaw, K. S., Dobbie, S., O'Sullivan, D., and Malkin, T. L.: The importance of feldspar for ice nucleation by mineral dust in mixed-phase clouds, Nature, 498, 355-358, 2013.

Baddock, M. C., Bullard, J. E., and Bryant, R. G.: Dust source identification using MODIS: A comparison of techniques applied to the Lake Eyre Basin, Australia, Remote Sens. Environ., 113, 1511-1528, 2009.

Baddock, M. C., Ginoux, P., Bullard, J. E, and Gill, T. E.: Do MODIS-defined dust sources have a geomorphological signature?, Geophys. Res. Lett., 43, 2606-2613, doi:10.1002/2015GL067327, 2016.

Bryant, R. G., Bigg, G. R., Mahowald, N. M., Eckardt, F. D., and Ross, S. G.: Dust emission response to climate in southern Africa, J. Geophys. Res., 112, D09207, doi:10.1029/2005JD007025, 2007.

Bullard, J., Baddock, M., McTainsh, G., and Leys, J.: Sub-basin scale dust source geomorphology detected using MODIS, Geophys. Res. Lett., 35, L15404, doi:10.1029/2008GL033928, 2008.

Bullard, J. E., Harrison, S. P., Baddock, M. C., Drake, N., Gill, T. E., McTainsh, G., and Sun, Y.: Preferential dust sources: A geomorphological classification designed for use in global dust-cycle models, J. Geophys. Res.-Earth Surf., 116, F04034, doi:10.1029/2011JF002061, 2011.

Cahill, C. F.: Asian aerosol transport to Alaska during ACE-Asia, J. Geophys. Res.-Atmos., 108, 8664, doi:10.1029/2002JD003271, D23, 2003.

Channan, S., Collins, K., and Emanuel, W. R.: Global mosaics of the standard MODIS land cover type data, University of Maryland and the Pacific Northwest National Laboratory, College Park, Maryland, USA, 2014.

Creamean, J. M., Suski, K. J., Rosenfeld, D., Cazorla, A., DeMott, P. J., Sullivan, R. C., White, A. B., Ralph, F. M., Minnis, P., Comstock, J. M., Tomlinson, J. M., and Prather, K. A.: Dust and biological aerosols from the Sahara and Asia influence precipitation in the western US, Science, 339, 1572-1578, 2013.

Darmenova, K., Sokolik, I. N., and Darmenov, A.: Characterization of east Asian dust outbreaks in the spring of 2001 using ground-based and satellite data, J. Geophys. Res.-Atmos., 110, D02204, doi:10.1029/2004JD004842, 2005.

Atmos. Chem. Phys. Discuss., doi:10.5194/acp-2016-681, 2016
Manuscript under review for journal Atmos. Chem. Phys.
Published: 10 October 2016

Atmospheric Chemistry and Physics
Discussions
Open Access

DeSouza‐Machado S. G., Strow, L. L., Imbiriba, B., McCann, K., Hoff, R. M., Hannon, S. E., Martins, J. V., Tanré, D., Deuzé, J. L., Ducos, F., and Torres, O.: Infrared retrievals of dust using AIRS: Comparisons of optical depths and heights derived for a North African dust storm to other collocated EOS A‐Train and surface observations, J. Geophys. Res.-Atmos., 115, D15201, doi:10.1029/2009JD012842, 2010.

Deuzé, J. L., Bréon, F. M., Devaux, C., Goloub, P., Herman, M., Lafrance, B., Maignan, F., Marchand, A., Nadal, F., Perry, G., and Tanré D.: Remote sensing of aerosols over land surfaces from POLDER‐ADEOS‐1 polarized measurements, J. Geophys. Res.-Atmos., 106(D5), 4913-4926, doi:10.1029/2000JD900364, 2001.

Di Pierro, M., Jaeglé, L., and Anderson, T. L.: Satellite observations of aerosol transport from East Asia to the Arctic: three case studies, Atmos. Chem. Phys., 11, 2225-2243, doi:10.5194/acp-11-2225-2011, 2011.

Dickerson, R. R., Li, C., Li, Z., Marufu, L., Stehr, J., McClure, B., Krotkov, N., Chen, H., Wang, P., Xia, X., Ban, X., Gong, F., Yuan, J., and Yang, J.: Aircraft observations of dust and pollutants over northeast China: Insight into the meteorological mechanisms of transport, J. Geophys. Res.-Atmos., 112, D24S90, doi:10.1029/2007JD008999, 2007.

Ding, R., Li, J., Wang, S., and Ren, F.: Decadal change of the spring dust storm in northwest China and the associated atmospheric circulation, Geophys. Res. Lett., 32, L02808, doi:10.1029/2004GL021561, 2005.

Draxler, R. R., Ginoux, P., and Stein, A. F.: An empirically derived emission algorithm for wind-blown dust, J. Geophys. Res.-Atmos., 115, D16212, doi:10.1029/2009JD013167, 2010.

Eckardt, F. D., and Kuring, N.: SeaWiFS identifies dust sources in the Namib Desert, Int. J. Remote Sens., 26(19), 4159-4167, 2005.

Engelstaedter, S., and Washington, R.: Temporal controls on global dust emissions: The role of surface gustiness, Geophys. Res. Lett., 34, L15805, doi:10.1029/2007GL029971, 2007.

Formenti, P., Rajot, J. L., Desboeufs, K., Saïd, F., Grand, N., Chevaillier, S., and Schmechtig, C.: Airborne observations of mineral dust over western Africa in the summer Monsoon season: spatial and vertical variability of physico-chemical and optical properties, Atmos. Chem. Phys., 11, 6387-6410, doi:10.5194/acp-11-6387-2011, 2011a.

Formenti, P., Schütz, L., Balkanski, Y., Desboeufs, K., Ebert, M., Kandler, K., Petzold, A., Scheuvens, D., Weinbruch, S., and Zhang, D.: Recent progress in understanding physical and chemical properties of African and Asian mineral dust, Atmos. Chem. Phys., 11, 8231-8256, doi:10.5194/acp-11-8231-2011, 2011b.

Gao, H., and Washington, R.: Arctic oscillation and the interannual variability of dust emissions from the Tarim Basin: a TOMS AI based study, Clim. Dynam., 35, 511-522, 2010.

Gao, T., Han, J., Wang, Y., Pei, H., and Lu, S.: Impacts of climate abnormality on remarkable dust storm increase of the Hunshdak Sandy Lands in northern China during 2001–2008, Meteorol. Appl., 19, 265-278, 2012.

Gillette, D. A.: A qualitative geophysical explanation for hot spot dust emitting source

Atmos. Chem. Phys. Discuss., doi:10.5194/acp-2016-681, 2016
Manuscript under review for journal Atmos. Chem. Phys.
Published: 10 October 2016

regions, Contrib. Atmos. Phys., 72(1), 67-77, 1999.

Ginoux, P., Chin, M., Tegen, I., Prospero, J., Holben, B., Dubovik, O., and Lin, S.: Sources and distributions of dust aerosols simulated with the GOCART model, J. Geophys. Res.-Atmos., 106(D17), 20255-20273, doi:10.1029/2000JD000053, 2001.

Ginoux, P., Prospero, J. M, Gill, T. E., Hsu, C. H., Zhao, M.: Global-scale attribution of anthropogenic and natural dust sources and their emission rates based on MODIS Deep Blue aerosol products, Rev. Geophys., 50, RG3005, doi:10.1029/2012RG000388, 2012.

Gong, S. L., Zhang, X. Y., Zhao, T. L., McKendry, I., Jaffe, D., and Lu, N.: Characterization of soil dust aerosol in China and its transport and distribution during 2001 ACE - Asia: 2. Model simulation and validation, J. Geophys. Res.-Atmos., 108, 4262, doi:10.1029/2002JD002633, D9, 2003.

Goudie, A. Desert dust and human health disorders, Environ. Int., 63, 101-113, 2014.

Guan, Q., Yang, J., Zhao, S., Pan, B., Liu, C., Zhang, D., and Wu, T.: Climatological analysis of dust storms in the area surrounding the Tengger Desert during 1960-2007, Clim. Dynam., 45, 903-913, 2015.

Han, Y., Fang, X., Kang, S., Wang, H., and Kang, F.: Shifts of dust source regions over central Asia and the Tibetan Plateau: Connections with the Arctic oscillation and the westerly jet, Atmos. Environ., 42, 2358-2368, 2008.

Hara, Y., Uno, I., and Wang, Z.: Long-term variation of Asian dust and related climate factors, Atmos. Environ., 40, 6730-6740, 2006.

Haustein, K., Washington, R., King, J., Wiggs, G., Thomas, D., Eckardt, F., Bryant, R., and Menut, L.: Testing the performance of state-of-the-art dust emission schemes using DO4Models field data, Geosci. Model. Dev., 8, 341-362, doi:10.5194/gmd-9-341-2015, 2015.

Heinold, B., Tegen, I., Schepanski, K., and Banks, J.: New developments in the representation of Saharan dust sources in the aerosol-climate model ECHAM6-HAM2, Geosci. Model. Dev., 9, 765-777, doi:10.5194/gmd-9-765-2016, 2016.

Huang, J., Minnis, P., Lin, B., Wang, T., Yi Y., Hu, Y., Sun-Mack, S., and Ayers, K.: Possible influences of Asian dust aerosols on cloud properties and radiative forcing observed from MODIS and CERES, Geophys. Res. Lett., 33, L06824, doi:10.1029/2005GL024724, 2006.Huang, J., Minnis, P., Lin, B., Wang, T., Yi, Y., Hu, Y., Sun-Mack, S., and Ayers, K.: Possible influences of Asian dust aerosols on cloud properties and radiative forcing observed from MODIS and CERES, Geophys. Res. Lett., 33, L06824, doi:10.1029/2005GL024724, 2006.

Huang, Z., Huang, J., Hayasaka, T., Wang, S., Zhou, T., and Jin H.: Short-cut transport path for Asian dust directly to the Arctic: a case study, Environ. Res. Lett., 10, 114018, 2015.

Jafari, R., and Malekian, M.: Comparison and evaluation of dust detection algorithms using MODIS Aqua/Terra Level 1B data and MODIS/OMI dust products in the Middle East, Int. J. Remote Sens., 36, 597-617, 2015.

Jia, R., Liu, Y., Chen, B., Zhang, Z., and Huang J.: Source and transportation of summer dust over the Tibetan Plateau, Atmos. Environ., 123, 210-219, 2015.

Atmos. Chem. Phys. Discuss., doi:10.5194/acp-2016-681, 2016
Manuscript under review for journal Atmos. Chem. Phys.
Published: 10 October 2016

Kalashnikova, O. V., Kahn, R., Sokolik, I. N., and Li, W.: Ability of multiangle remote sensing observations to identify and distinguish mineral dust types: Optical models and retrievals of optically thick plumes, J. Geophys. Res.-Atmos., 110, D18S14, doi:10.1029/2004JD004550, 2005.

Kang, L., Huang, J., Chen, S., and Wang X.: Long-term trends of dust events over Tibetan Plateau during 1961-2010, Atmos. Environ., 125, 188-198, 2016.

Kang, J.-Y.: Implementation of dust emission schemes into WRF/Chem, PhD thesis, Seoul National University, 2011.

Karimi, N., Moridnejad, A., Golian, S., Samani, J., Karimi, D., and Javadi, S.: Comparison of dust source identification techniques over land in the Middle East region using MODIS data, Can. J. Remote Sens., 38(5), 586-599, 2012.

Kim, C. H., and Lee, H. J.: Numerical simulations of Asian dust events: A Lagrangian Dust Model and its applications, Asia. Pac. J. Atmos. Sci., 49, 571-586, 2013.

Klüser, L., Martynenko, D., and Holzer-Popp, T.: Thermal infrared remote sensing of mineral dust over land and ocean: a spectral SVD based retrieval approach for IASI, Atmos. Meas. Tech., 4,757-773, 2011.

Knippertz, P., and Stuut, J.: Mineral Dust: A Key Player in the Earth System, Springer, 1-14, 2014.

Knippertz, P., and Todd, M. C.: The central west Saharan dust hot spot and its relation to African easterly waves and extratropical disturbances, J. Geophys. Res.-Atmos., 115, D12117, doi:10.1029/2009JD012819, 2010.

Kok, J. F., Mahowald, N. M., Fratini, G., Gillies, J. A., Ishizuka, M., Leys, J. F., Mikami, M., Park, M.-S., Park, S.-U., Van Pelt, R. S., and Zobeck, T. M.: An improved dust emission model – Part 1: Model description and comparison against measurements, Atmos. Chem. Phys., 14, 13023-13041, doi:10.5194/acp-14-13023-2014, 2014.

Kondratiev, I. I., and Skalyga, O. R.: Atmospheric transboundary transport of cesium-137 with terrigenous dust from Asian deserts to the southern Far East, Geography and Natural Resources, 32, 126-131, 2011.

Koven, C. D., and Fung, I.: Identifying global dust source areas using high-resolution land surface form, J. Geophys. Res., 113, D22204, doi:10.1029/2008JD010195, 2008.

Ku, B., and Park, R. J.: Inverse modeling analysis of soil dust sources over East Asia, Atmos. Environ., 45, 5903-5912, 2011.

Kurosaki, Y., and Mikami, M.: Recent frequent dust events and their relation to surface wind in East Asia, Geophys. Res. Lett., 30, 1736, doi:10.1029/2003GL017261, 2003.

Kurosaki, Y., Shinoda, M., and Mikami, M.: What caused a recent increase in dust outbreaks over East Asia?, Geophys. Res. Lett., 38, L11702, doi:10.1029/2011GL047494, 2011.

Laurent, B., Marticorena, B., Bergametti, G., Chazette, P., Maignan, F., and Schmechtig, C.: Simulation of the mineral dust emission frequencies from desert areas of China and Mongolia using an aerodynamic roughness length map derived from the POLDER/ADEOS 1 surface products, J. Geophys. Res., 110, D18S04, doi:10.1029/2004JD005013, 2005.

Lee, E. H., and Sohn, B. J.: Recent increasing trend in dust frequency over Mongolia and Inner Mongolia regions and its association with climate and surface condition change,

Atmos. Chem. Phys. Discuss., doi:10.5194/acp-2016-681, 2016
Manuscript under review for journal Atmos. Chem. Phys.
Published: 10 October 2016

Atmospheric Chemistry and Physics Discussions

Atmos. Environ., 45, 4611-4616, 2011.

Lee, J. A., Baddock, M. C., Mbuh, M. J., and Gill, T. E.: Geomorphic and land cover characteristics of aeolian dust sources in West Texas and eastern New Mexico, USA, Aeolian Res., 3, 459-466, 2012.

Lee, Y. G., Kim, J., Ho, C. H., An, S., Cho, H., Mao, R., Tian, B., Wu, D., Lee, J. N., Kalashnikova, O., Choi, Y., Yeh, S.: The effects of ENSO under negative AO phase on spring dust activity over northern China: an observational investigation, Int. J. Climatol., 35, 935-947 2015.

Li, B. G., Ma, L. C., Jiang, P. A., Duan, Z. Q., Sun, D. F., Qiu, H. L., Zhong, J. P., and Wu, H. Q.: High precision topographic data on Lop Nor basin's Lake "Great Ear" and the timing of its becoming a dry salt lake, Chinese Sci. Bull., 53, 905-914, 2008.

Li, D. and Zhong, H. L.: The climatic formation cause and the future developing trend of sand-dust storm in China, China Environ. Sci., 27, 14-18, 2007.

Littmann, T.: Dust storm frequency in Asia: climatic control and variability, Int. J. Climatol., 11, 393-412, 1991.

Lim, J. Y., and Chun, Y. The characteristics of Asian dust events in Northeast Asia during the springtime from 1993 to 2004, Global Planet. Change, 52, 231-247 2006.

Lary, D. J., Alavi, A, H., Gandomi, A. H., and Walker, A. L.: Machine learning in geosciences and remote sensing, Geoscience Frontiers, 7, 3-10, 2016.

Maher, B. A., Prospero, J. M., Mackie, D., Gaiero, D., Hesse, P. P., Balkanski, Y.: Global connections between aeolian dust, climate and ocean biogeochemistry at the present day and at the last glacial maximum, Earth-Sci. Rev., 99, 61-97, 2010.

Mahowald, N., Albani, S., Kok, J. F., Engelstaeder, S., Scanza, R., Ward, D. S., Flanner, M. G.: The size distribution of desert dust aerosols and its impact on the Earth system, Aeolian Res., 15, 53-71, 2014.

Mao, R., Ho, C. H., Shao, Y., Gong, D., and Kim J.: Influence of Arctic Oscillation on dust activity over northeast Asia, Atmos. Environ., 45, 326-337, 2011.

Miller, S. D.: A consolidated technique for enhancing desert dust storms with MODIS, Geophys. Res. Lett., 30, 2071, doi:10.1029/2003GL018279, 2003.

Mohammed, B. A. R.: Correlation between solar cycles and dust activity pver Iraq, J. Al. Narain Univ., 13, 82-87, 2010.

Natsagdorj, L., Jugder, D., and Chung, Y. S.: Analysis of dust storms observed in Mongolia during 1937-1999, Atmos. Environ., 37, 1401-1411, 2003.

Nobakht, M., Shahgedanova, M., and White, K.: High resolution mapping of dust sources in Central Asia using MODIS imagery, EGU General Assembly Conference Abstracts, 17, 7567, 2015.

Parajuli, S. P., Yang, Z. L., and Kocurek, G.: Mapping erodibility in dust source regions based on geomorphology, meteorology, and remote sensing, J. Geophys. Res.-Earth Surf., 119, 1977-1994, doi:10.1002/2014JF003095, 2014.

Park, S. U., and In, H. J.: Parameterization of dust emission for the simulation of the yellow sand (Asian dust) event observed in March 2002 in Korea, J. Geophys. Res.-Atmos., 108, 4618, doi:10.1029/2003JD003484, 2003.

Park, S. U., Choe, A., Lee, E. H., Park, M. S., Song X.: The Asian dust aerosol model 2 (ADAM2) with the use of normalized difference vegetation index (NDVI) obtained

Atmos. Chem. Phys. Discuss., doi:10.5194/acp-2016-681, 2016
Manuscript under review for journal Atmos. Chem. Phys.
Published: 10 October 2016

from the Spot4/vegetation data, Theor. Appl. Climatol., 101, 191-208, 2010.

Pérez, C., Haustein, K., Janjic, Z., Jorba, O., Huneeus, N., Baldasano, J. M., Black, T., Basart, S., Nickovic, S., Miller, R. L., Perlwitz, J. P., Schulz, M., and Thomson, M.: Atmospheric dust modeling from meso to global scales with the online NMMB/BSC-Dust model - Part 1: Model description, annual simulations and evaluation, Atmos. Chem. Phys., 11, 13001-13027, doi:10.5194/acp-11-13001-2011, 2011.

Perlwitz, J. P., Pérez García-Pando, C., and Miller, R. L.: Predicting the mineral composition of dust aerosols - Part 2: Model evaluation and identification of key processes with observations, Atmos. Chem. Phys., 15, 11629-11652, doi:10.5194/acp-15-11629-2015, 2015.

Prospero, J. M., Ginoux, P., Torres, O., Nicholson, S. E., and Gill, T. E.: Environmental characterization of global sources of atmospheric soil dust identified with the Nimbus 7 Total Ozone Mapping Spectrometer (TOMS) absorbing aerosol product, Rev. Geophys., *40*, 1002, doi:10.1029/2000RG000095, 2002.

Qian, Y.-B., Wu, Z.-N,. Yang, Q., Zhang, L.-Y., and Wang, X.-Y.: Ground-surface conditions of sand-dust event occurrences in the southern Junggar Basin of Xinjiang, China, J. Arid Environ., 70, 49-62, 2007.

Rivera, N. I. R., Gill, T. E., Bleiweiss, M. P., and Hand, J. L.: Source characteristics of hazardous Chihuahuan Desert dust outbreaks, Atmos. Environ., 44, 2457-2468, 2010.

Roskovensky, J. K., and Liou, K. N.: Differentiating airborne dust from cirrus clouds using MODIS data, Geophys. Res. Lett., 32, L12809, doi:10.1029/2005GL022798, 2005.

Sayer, A. M., Hsu, N. C., Bettenhausen, C., and Jeong M.-J.: Validation and uncertainty estimates for MODIS Collection 6 “Deep Blue” aerosol data, J. Geophys. Res.-Atmos., 118, 7864-7872, doi:10.1002/jgrd.50600, 2013.

Schepanski, K., Tegen, I., Todd, M. C., Heinold, B., Bönisch, G., Laurent, B., and Macke A.: Meteorological processes forcing Saharan dust emission inferred from MSG‐SEVIRI observations of subdaily dust source activation and numerical models, J. Geophys. Res., 114, D10201, doi:101029/2008JD010325, 2009.

Schepanski, K., Tegen, I., and Macke, A.: Comparison of satellite based observations of Saharan dust source areas, Remote Sens. Environ., 123, 90-97, 2012.

Shao, Y., Klose, M., and Wyrwoll, K.-H.: Recent global dust trend and connections to climate forcing, J. Geophys. Res. Atmos., 118, 11107-11118, doi:10.1002/jgrd.50836, 2013.

Shao, Y., Wyrwoll, K. H., Chappell, A., Huang, J., Lin, Z., McTainsh, G., Mikami, M., Tanaka, T. Y., Wang, X., and Yoon, S.: Dust cycle: An emerging core theme in Earth system science, Aeolian Res., 2, 181-204, 2011.

Solomos, S., Kallos, G., Kushta, J., Astitha, M., Tremback, C., Nenes, A., and Levin, Z.: An integrated modeling study on the effects of mineral dust and sea salt particles on clouds and precipitation, Atmos. Chem. Phys., 11, 873-892, doi:10.5194/acp-11-873-2011, 2011.

Sternberg, T., Rueff, H., and Middleton, N.: Contraction of the Gobi Desert, 2000-2012, Remote Sens., 7, 1346-1358, 2015.

Atmos. Chem. Phys. Discuss., doi:10.5194/acp-2016-681, 2016
Manuscript under review for journal Atmos. Chem. Phys.
Published: 10 October 2016

Takemi, T., and Seino, N.: Dust storms and cyclone tracks over the arid regions in east Asia in spring, J. Geophys. Res.-Atmos., 110, D18S11, doi:10.1029/2004JD004698, 2005.

Tan, M., Li, X., Xin, L.: Intensity of dust storms in China from 1980 to 2007: A new definition, Atmos. Environ., 85, 215-222, 2014.

Tanaka, T. Y., and Chiba, M.: A numerical study of the contributions of dust source regions to the global dust budget, Global Planet. Change, 52, 88-104, 2006.

Tao, S., Fang, J., Zhao, X., Zhao. S., Shen, H., Hu, H., Tang Z., Wang, Z., and Guo, Q.: Rapid loss of lakes on the Mongolian Plateau, P. Natl. Acad. Sci. USA, 112, 2281-2286, 2015.

Taramelli, A., Pasqui, M., Barbour, J., Kirschbaum, D., Bottai, L., Busillo, C., Calastrini, F., Guarnieri, F., and Small C.: Spatial and temporal dust source variability in northern China identified using advanced remote sensing analysis, Earth Surf. Proc. Land., 38, 793-809, 2013.

Tegen, I., and Fung, I.: Contribution to the atmospheric mineral aerosol load from land surface modification, J. Geophys. Res., 100, 18707-18726, doi:10.1029/95JD02051, 1995.

Tsai, F., Chen, G. T.-J., Liu, T.-H., Lin, W.-D., and Tu, J.-Y.: Characterizing the transport pathways of Asian dust, J. Geophys. Res., 113, D17311, doi:10.1029/2007JD009674, 2008.

Tsolmon, R., Ochirkhuyag, L., and Sternberg, T.: Monitoring the source of trans-national dust storms in north east Asia, Int. J. Digit. Earth, 1, 119-129, 2008.

Uno, I., Wang, Z., Chiba, M., Chun, Y. S., Gong, S. L., Hara, Y., Jung, E., Lee, S.-S., Liu, M., Mikami, M., Music, S., Nickovic, S., Satake, S., Shao, Y., Song, Z., Sugimoto, N., Tanaka, T., and Westphal, D. L.: Dust model intercomparison (DMIP) study over Asia: Overview, J. Geophys. Res., 111, D12213, doi:10.1029/2005JD006575, 2006.

Uno, I., Eguchi, K., Yumimoto, K., Takemura, T., Shimizu A., Uematsu, M., Liu, Z., Wang Z., Hara, Y., and Sugimoto, N.: Asian dust transported one full circuit around the globe, Nat. Geosci., 2, 557-560, 2009.

Varga, G.: Spatio-temporal distribution of dust storms-a global coverage using NASA Total Ozone Mapping Spectrometer aerosol measurements, Hungar. Geograph. Bull.,61, 275-298, 2012.

Vickery, K. J., Eckardt, F. D., and Bryant, R. G.: A sub‐basin scale dust plume source frequency inventory for southern Africa, 2005-2008, Geophys. Res. Lett., 40, 5274-5279, doi:10.1002/grl.50968, 2013.

Vinoj, V., Rasch, P. J., Wang, H., Yoon, J.-H., Ma, P.-L., Landu, K., and Singh B.: Short-term modulation of Indian summer monsoon rainfall by West Asian dust, Nat. Geosci., 7, 308-313, 2014.

Walker, A. L., Liu, M., Miller, S. D., Richardson, K. A., and Westphal, D. L.: Development of a dust source database for mesoscale forecasting in southwest Asia, J. Geophys. Res., 114, D18207, doi:10.1029/2008JD011541, 2009.

Waggoner, D. G., and Sokolik, I. N.: Seasonal dynamics and regional features of MODIS-derived land surface characteristics in dust source regions of East Asia, Remote Sens. Environ., 114, 2126-2136, 2010.

Atmos. Chem. Phys. Discuss., doi:10.5194/acp-2016-681, 2016
Manuscript under review for journal Atmos. Chem. Phys.
Published: 10 October 2016

Atmospheric Chemistry and Physics Discussions

Wang, G., Tuo, W., and Du, M.: Flux and composition of wind-eroded dust from different landscapes of an arid inland river basin in north-western China, J. Arid Environ., 58, 373-385, 2004.

Wang, K., Zhang, Y., Nenes, A., and Fountoukis, C.: Implementation of dust emission and chemistry into the Community Multiscale Air Quality modeling system and initial application to an Asian dust storm episode, Atmos. Chem. Phys., 12, 10209-10237, doi:10.5194/acp-12-10209-2012, 2012.

Wang, J., Christopher, S. A., Reid, J. S., Maring, H., Savoie, D., Holben, B., Livingston, J. M., Russell, P. B., Yang, S.-K.: GOES 8 retrieval of dust aerosol optical thickness over the Atlantic Ocean during PRIDE, J. Geophys. Res., 108, 8595, doi:10.1029/2002JD002494, 2003.

Wang, S., Wang, J., Zhou, Z., and Shang K.: Regional characteristics of three kinds of dust storm events in China, Atmos. Environ., 39, 509-520, 2005.

Wang, T., Yan, C. Z., Song, X. and Li, S.: Landsat images reveal trends in the aeolian desertification in a source area for sand and dust storms in China's Alashan Plateau (1975–2007), Land Degrad. Dev., 24, 422-429, doi:10.1002/ldr.1138, 2013.

Wang, X., Huang, J., Ji, M., and Higuchi, K.: Variability of East Asia dust events and their long-term trend, Atmos. Environ., 42, 3156-3165, 2008.

Wang, X., Zhou, Z., and Dong, Z.: Control of dust emissions by geomorphic conditions, wind environments and land use in northern China: An examination based on dust storm frequency from 1960 to 2003, Geomorphology, 81, 292-308, 2006.

Washington, R., Todd, M., Middleton, N. J., and Goudie, A. S.: Dust-storm source areas determined by the total ozone monitoring spectrometer and surface observations, Ann. Assoc. Am. Geogr., 93, 297-313, 2003.

Xin, X., Sokolik, I. N.: Seasonal dynamics of threshold friction velocity and dust emission in Central Asia, J. Geophys. Res.-Atmos., 120, 1536-1564, doi:10.1002/2014JD022471, 2015.

Xu, C., Ma, Y. M., You, C., and Zhu, Z. K.: The regional distribution characteristics of aerosol optical depth over the Tibetan Plateau, Atmos. Chem. Phys., 15, 12065-12078, doi:10.5194/acp-15-12065-2015, 2015.

Xuan, J., Sokolik, I. N., Hao, J., Guo, F., Mao, H., and Yang, G.: Identification and characterization of sources of atmospheric mineral dust in East Asia, Atmos. Environ., 38, 6239-6252, 2004.

Yang, L., Yue, L., and Li Z.: The influence of dry lakebeds, degraded sandy grasslands and abandoned farmland in the arid inlands of northern China on the grain size distribution of East Asian aeolian dust, Environ. Geol., 53, 1767-1775, 2008.

Yang, X., Shen, S., Yang, F., He, Q., Ali, M., Huo, W., Liu, X.: Spatial and temporal variations of blowing dust events in the Taklimakan Desert, Theor. Appl. Climatol., 1-9, doi: 10.1007/s00704-015-1537-4, 2015.

Yao, Z., Xiao, J., Li, C., and Zhu, K.: Regional characteristics of dust storms observed in the Alxa Plateau of China from 1961 to 2005, Environ. Earth Sci., 64, 255-267, 2011.

Zhang, B., Tsunekawa, A., and Tsubo, M.: Contributions of sandy lands and stony deserts to long-distance dust emission in China and Mongolia during 2000-2006, Global Planet. Change, 60, 487-504, 2008.

Atmos. Chem. Phys. Discuss., doi:10.5194/acp-2016-681, 2016
Manuscript under review for journal Atmos. Chem. Phys.
Published: 10 October 2016

Atmospheric Chemistry and Physics Discussions

Zhang, B., Tsunekawa, A., and Tsubo. M.: Identification of Dust Hot Spots from Multi-Resolution Remotely Sensed Data in Eastern China and Mongolia, Water Air Soil Poll., 226, 1-18, 2015a.

Zhang, P., Lu, N., Hu, X., and Dong, C.: Identification and physical retrieval of dust storm using three MODIS thermal IR channels, Global Planet. Change, 52, 197-206, 2006.

Zhang, X. L., Wu, G. J., Zhang, C. L., Xu, T. L., and Zhou, Q. Q.: What is the real role of iron oxides in the optical properties of dust aerosols?, Atmos. Chem. Phys., 15, 12159-12177, doi:10.5194/acp-15-12159-2015, 2015b.

Zhang, X. L., Zhou, Q. Q., Chen, W. W., Wang, Y. Y., and Tong, D. Q.: Observation and modeling of black soil wind-blown erosion from cropland in Northeastern China, Aeolian Res., 19, 153-162, 2015c.

Zhu, C., Wang, B., and Qian, W.: Why do dust storms decrease in northern China concurrently with the recent global warming?, Geophys. Res. Lett., 35, L18702, doi:10.1029/2008GL034886, 2008.